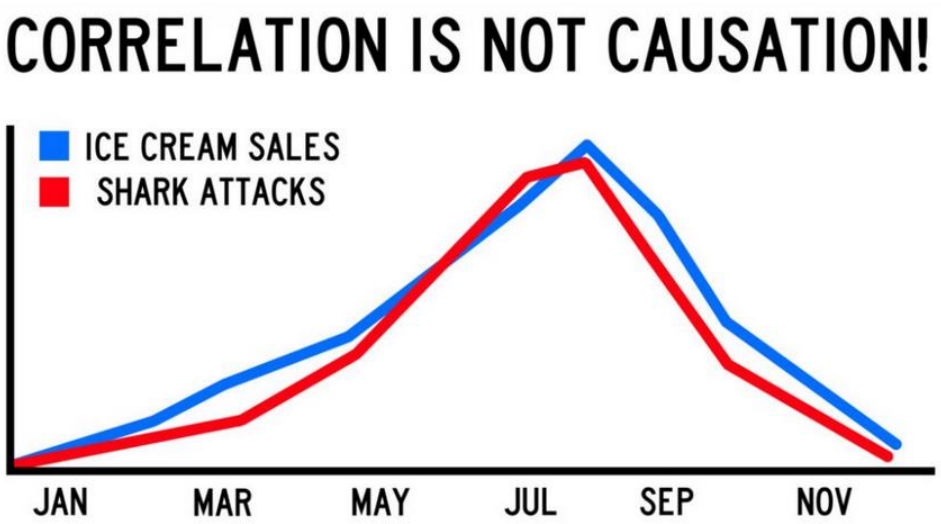
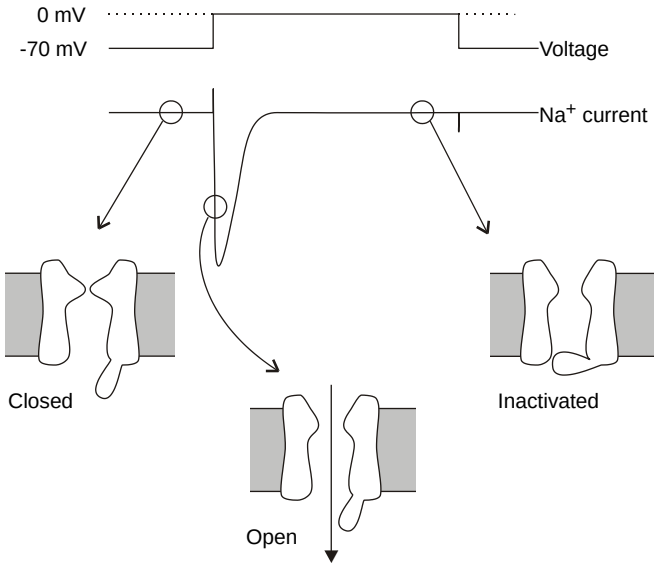
Experimental Approaches to Ion Channel Biophysics

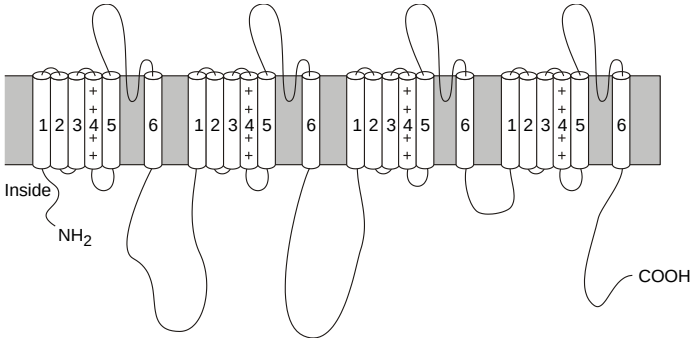
How do we interpret experimental results?

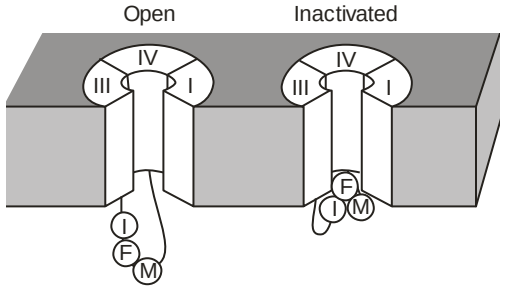


Inactivation- Na Channels

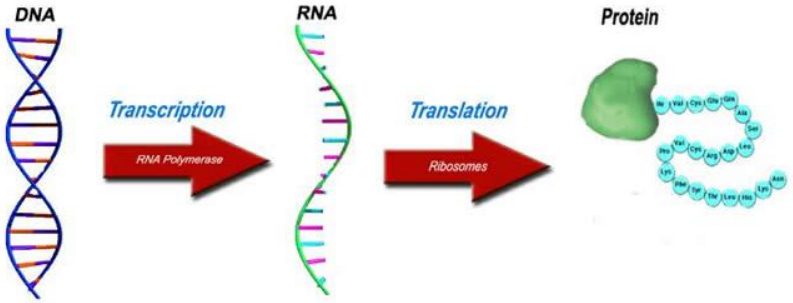
- Na channels inactivate to prevent continued depolarisation during AP
- Inactivation is distinct from pore closure.
- Hydrophobic linker (IFM) in III-IV repeat is responsible.
- Mutations in this linker can alter inactivation cause a disease “LQT syndrome” – why?

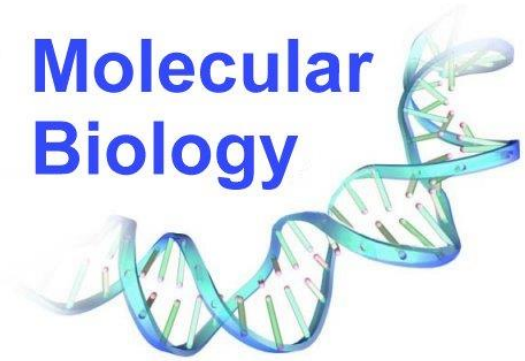


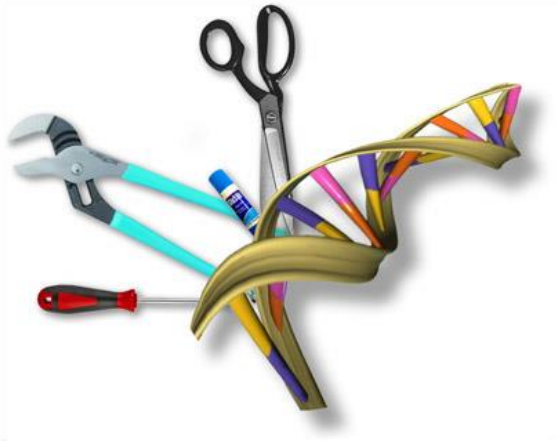




$$C_m \frac{dV}{dt} = -g_L (V - V_L) - \overline{g}_{Na} m^3 h (V - V_{Na}) - \overline{g}_K n^4 (V - V_K)$$







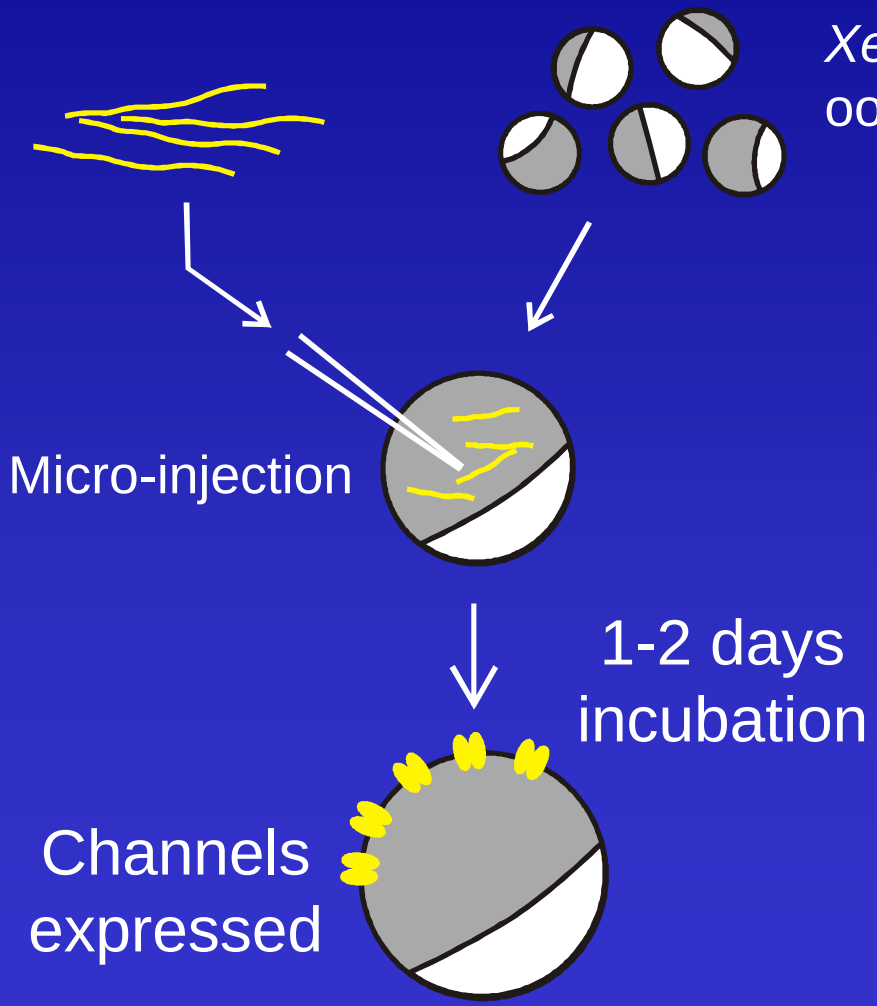
Can change any part of a protein and then study its altered properties

Xenopus laevis expression system

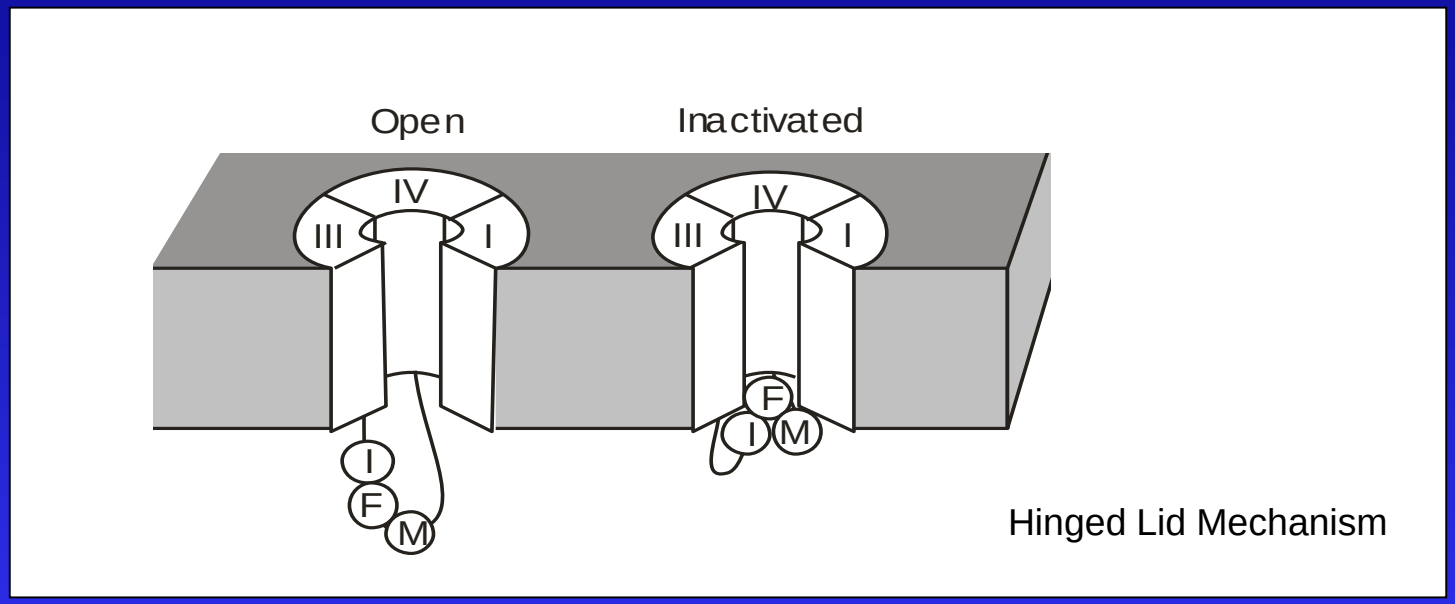
K^+ Channel gene → mRNA

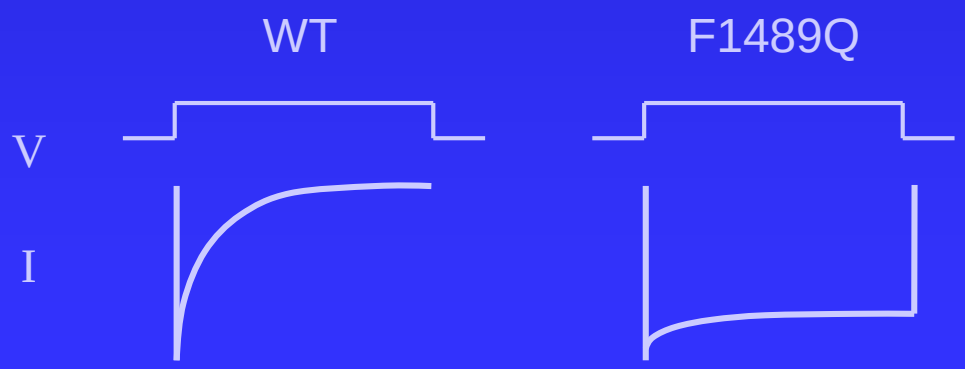


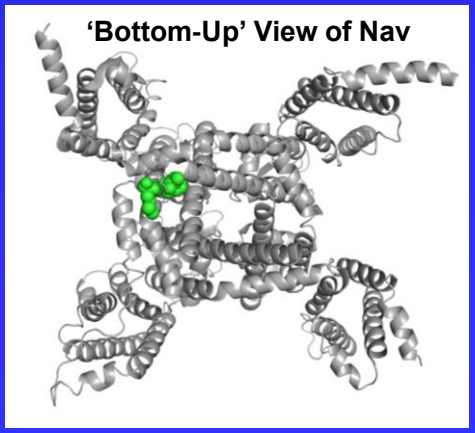




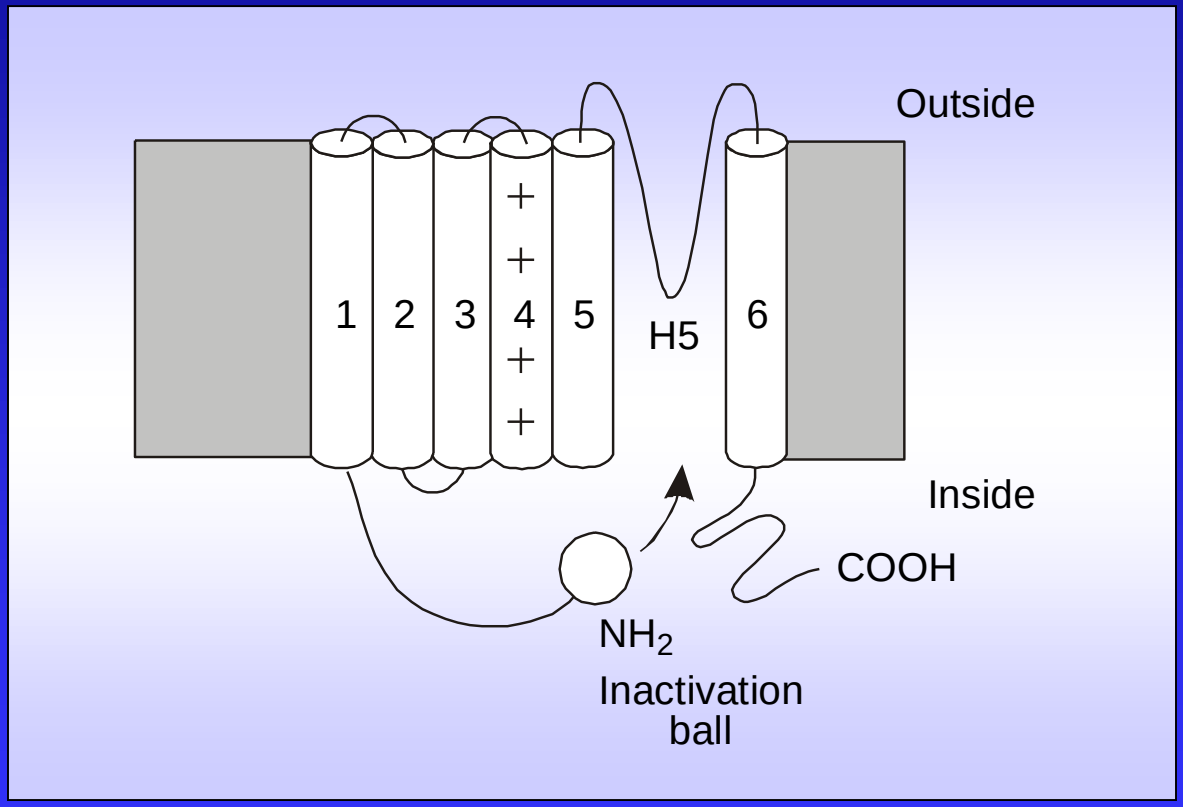
Na Channel Inactivation involves hydrophobic residues in III-IV Linker





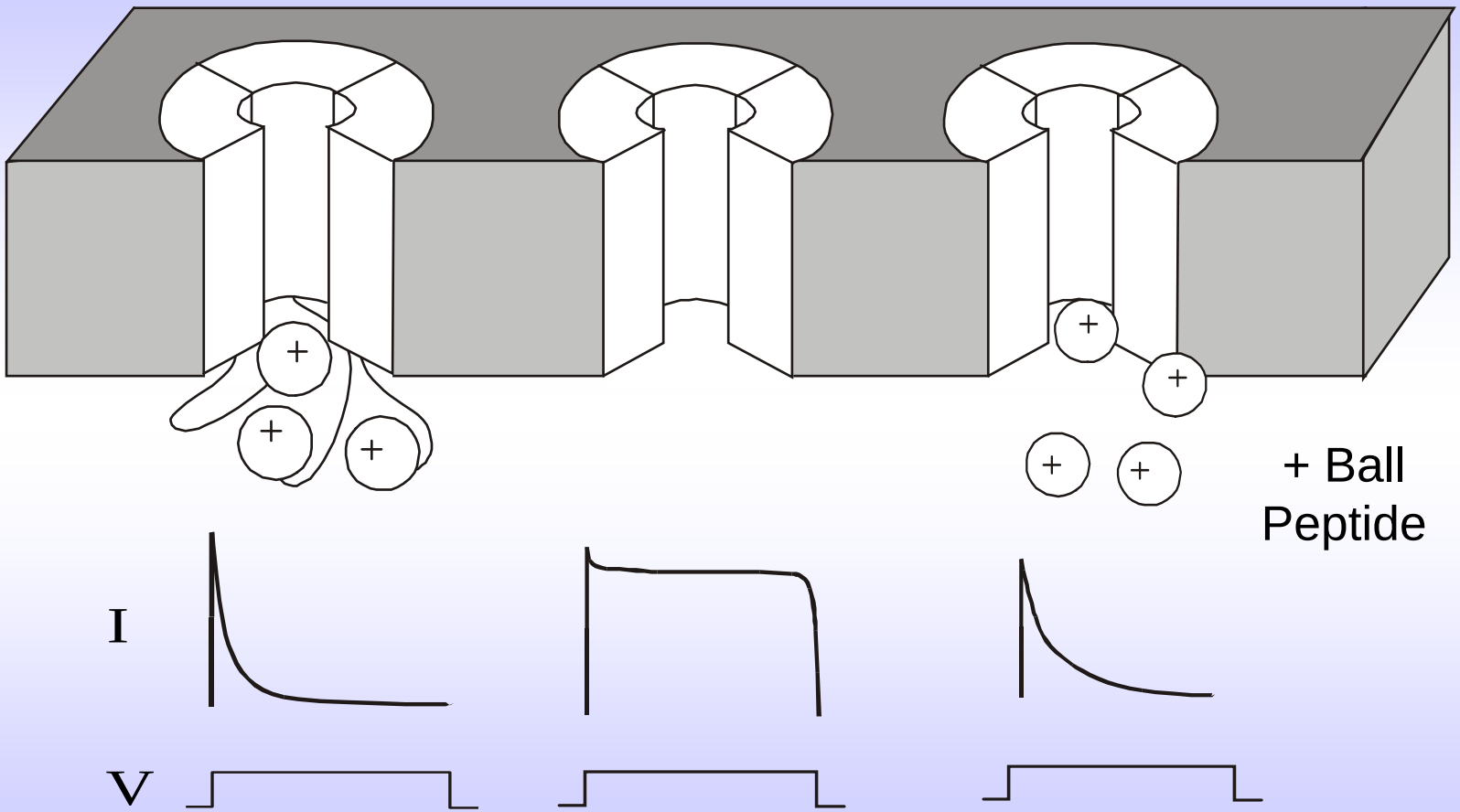


Different (but related) Mechanism of Channel Inactivation: SOME (but not all) K^+ Channels also inactivate using the 'BALL AND CHAIN' MECHANISM

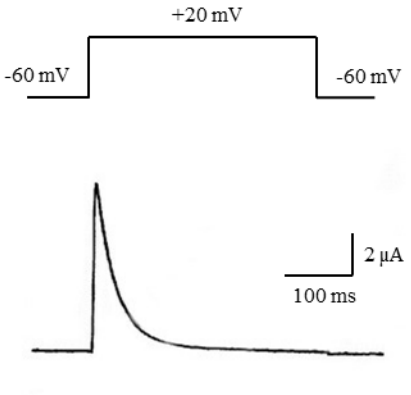


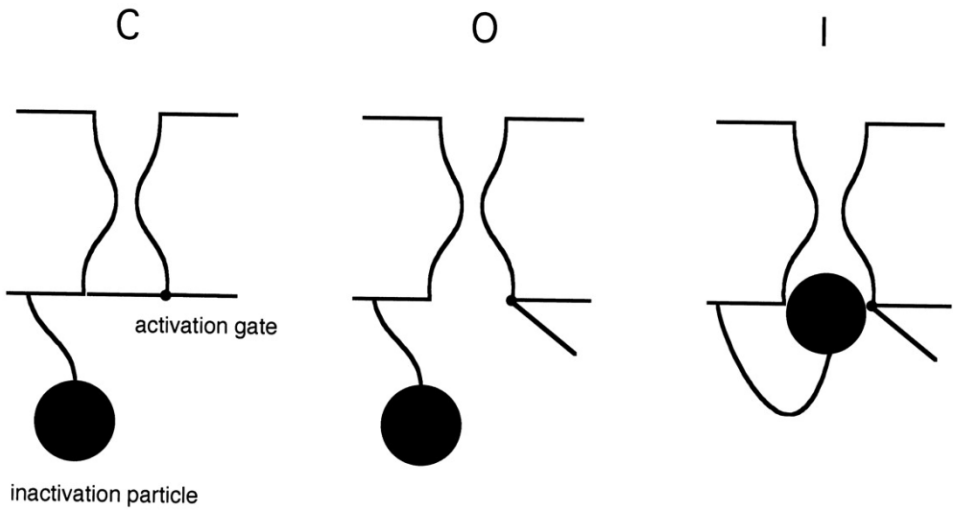
BALL (N-terminus) PHYSICALLY PLUGS THE PORE
Helps close K^+ channels quickly in 'fast-firing' neurons

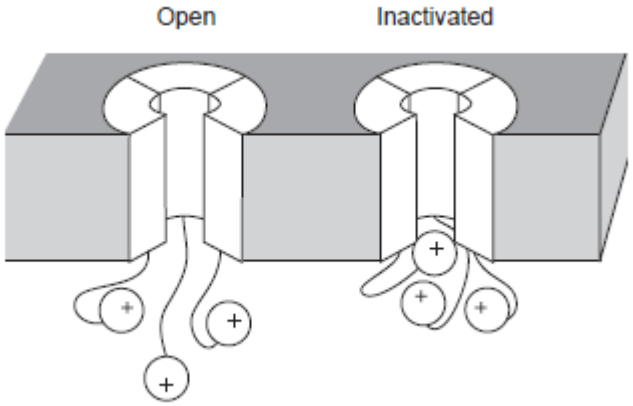
DISSECTING BALL AND CHAIN MECHANISM



Inactivation in '*Shaker*' Voltage-Gated K^+ Channels







(Science, 1990)

Biophysical and Molecular Mechanisms of *Shaker* Potassium Channel Inactivation

TOSHINORI HOSHI, WILLIAM N. ZAGOTTA, RICHARD W. ALDRICH*

- Inactivation involves an intracellular ‘particle’ that can be removed (by enzymes)
- Genetic deletion of the N-terminus of protein also removes inactivation
- Particle is ‘ball’ at end of N-terminus – attached to flexible ‘chain’ (all part of the protein)
- Positive charges in ‘ball’ particle are important for inactivation

Also a second paper (Science, 1990)

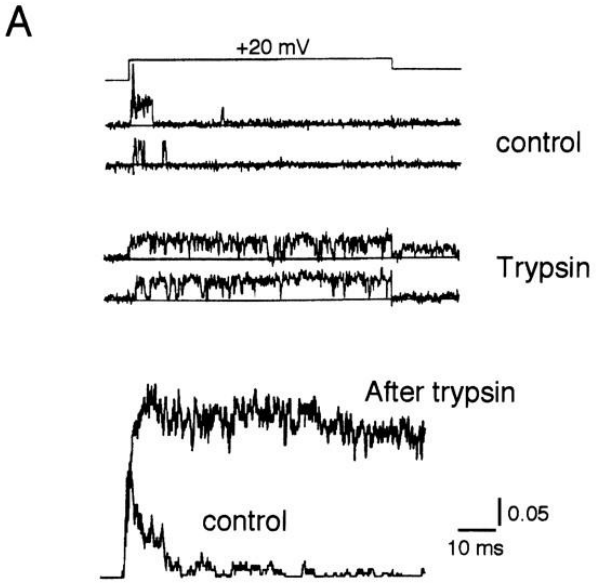
Restoration of Inactivation in Mutants of *Shaker* Potassium Channels by a Peptide Derived from ShB

WILLIAM N. ZAGOTTA, TOSHINORI HOSHI, RICHARD W. ALDRICH*

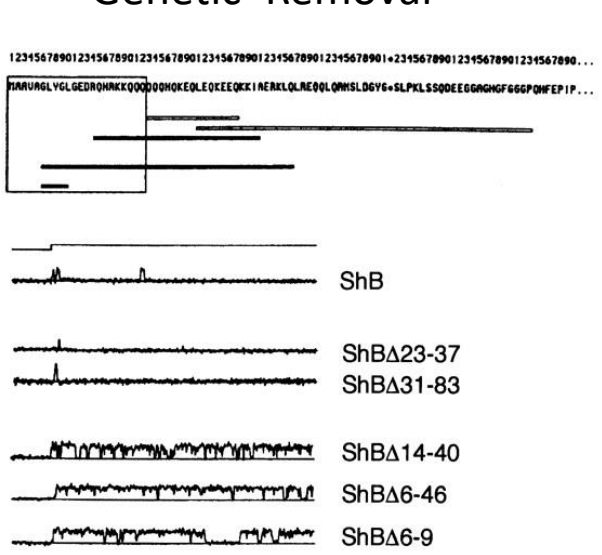
- Adding the ball back restores inactivation

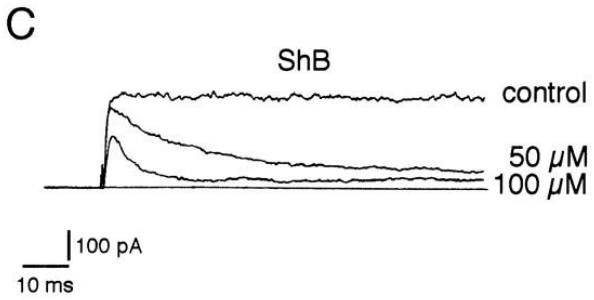
The Key Experiments which Demonstrate Molecular Mechanism of N-Type Inactivation

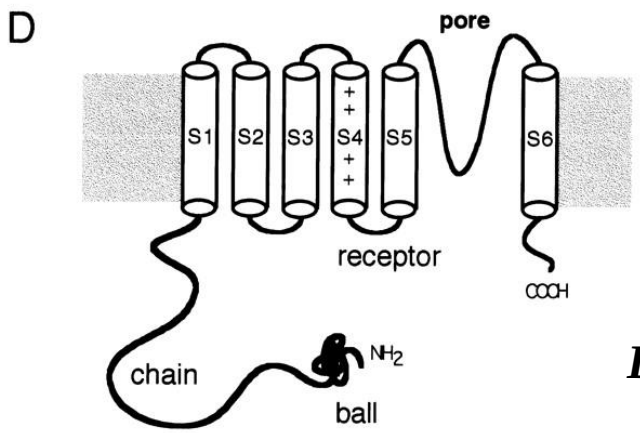
Enzymatic Removal



'Genetic' Removal







Can you add it back?

Ball and Chain Mechanism

(Science, 1993)

Functional Stoichiometry of Shaker Potassium Channel Inactivation

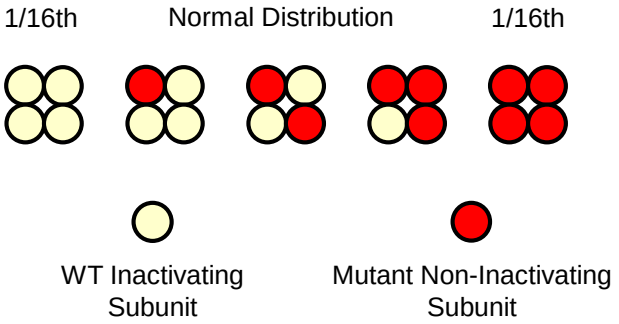
Roderick MacKinnon,* Richard W. Aldrich, Alice W. Lee

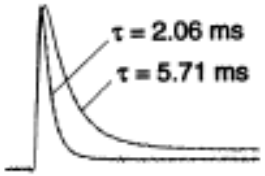
Shaker potassium channels from *Drosophila* are composed of four identical subunits. The contribution of a single subunit to the inactivation gating transition was investigated. Channels carrying a specific mutation in a single subunit can be labeled in a heterogeneous population and studied quantitatively with scorpion toxin sensitivity as a selection tag. Linkage within a single subunit of a mutation that removes the inactivation gate to a second mutation that affects scorpion toxin sensitivity demonstrates that only a single gate is necessary to produce inactivation. The inactivation rate constant for channels with a single gate was one-fourth that of channels with four gates. In contrast, the rate of recovery from inactivation was independent of the number of gates. It appears that each of the four open inactivation gates in a Shaker potassium channel is independent, but only one of the four gates closes in a mutually exclusive manner.

SCIENCE • VOL. 262 • 29 OCTOBER 1993 REPORTS

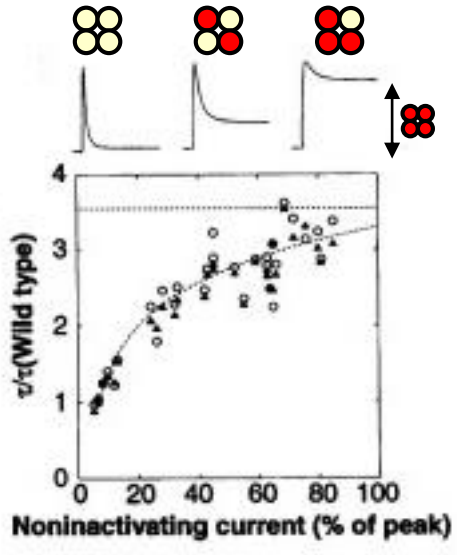
Functional Stoichiometry of Shaker Potassium Channel Inactivation

Roderick MacKinnon,* Richard W. Aldrich, Alice W. Lee

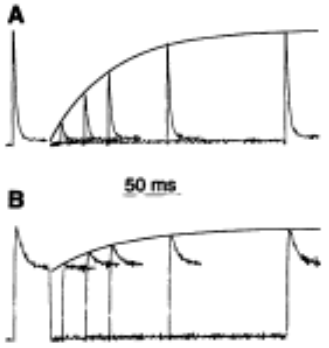




Open ⇌ Inactivated



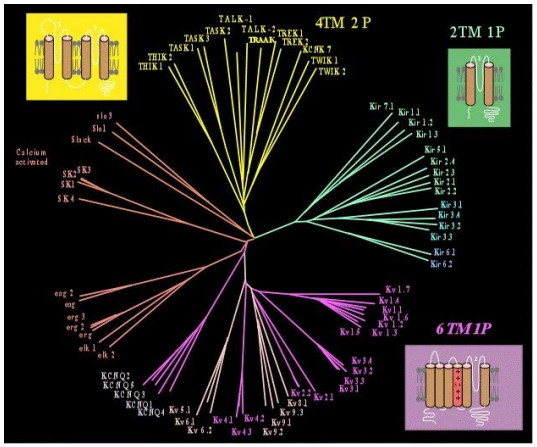
Macroscopic Currents from 'Mixed' Populations

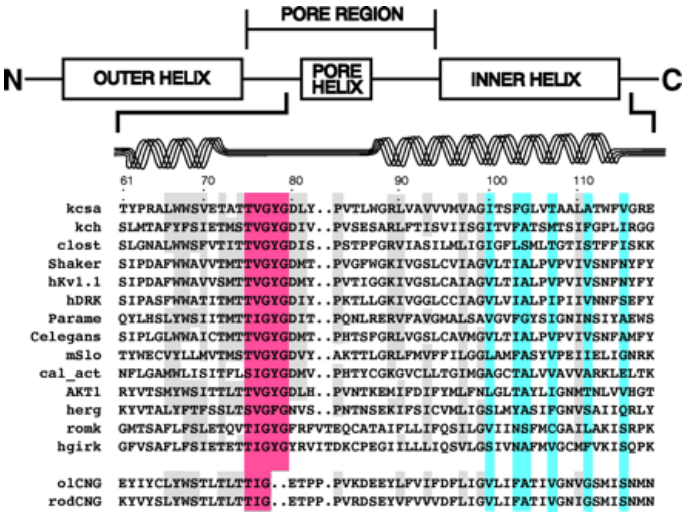


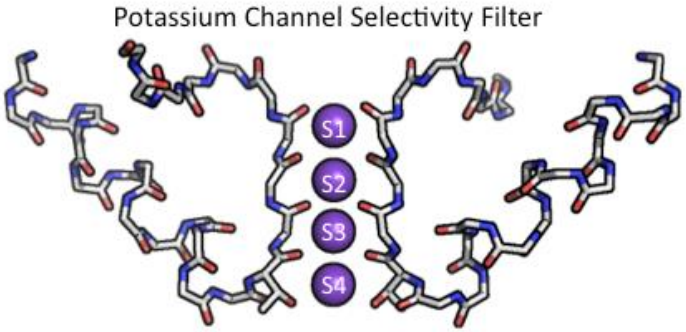
Off-rate does not depend on No of 'balls'

Fast Inactivation kinetics correlate with proportion of WT subunits
i.e. 'On-rate' depends on No of 'balls'

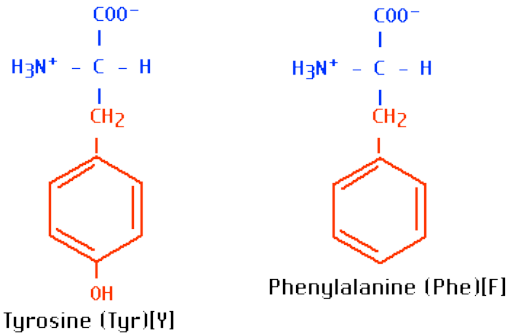
K^+ Ion Selectivity







TxGYG



Delocalised Electrons – could coordinate a K+ ion (cation:π Interaction)

Biophysical Journal Volume 66 April 1994 1061–1067

Mutations in the K^+ Channel Signature Sequence

Lise Heginbotham, Zhe Lu, Tatiana Abramson, and Roderick MacKinnon
Department of Neurobiology, Harvard Medical School, Boston, Massachusetts 02115



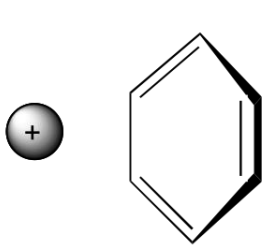
	1	2	3	4	5	6	7	8
	T	M	T	T	V	G	Y	G
A. selective	S	G I N	A S	A G N S	C L T		F V	
B. nonselective	G				A G N Q	A C P Q S		A C P Q S
C. gating currents only							A P	
D. do not express	A V		G N		E	E		

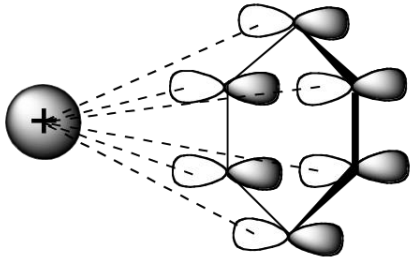
REPORTS

(Science, 1998)

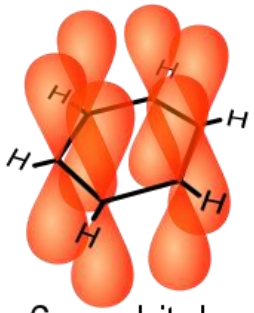
A Mechanism for Ion Selectivity in Potassium Channels: Computational Studies of Cation-π Interactions

Robert A. Kumpf and Dennis A. Dougherty*

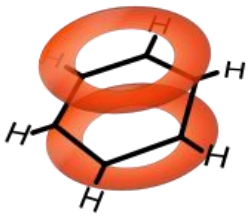




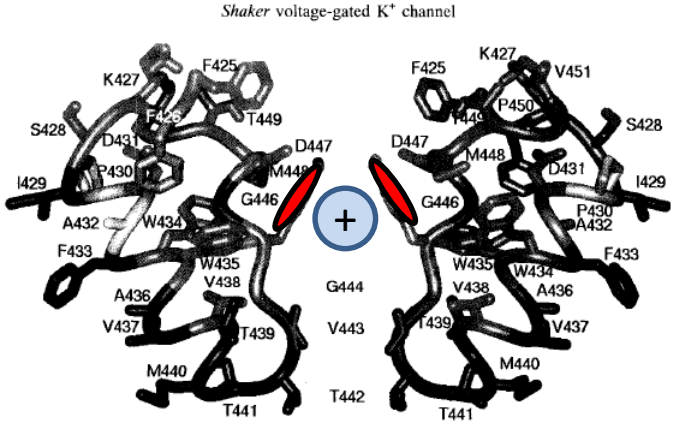
Benzene



6 p-orbitals



delocalized



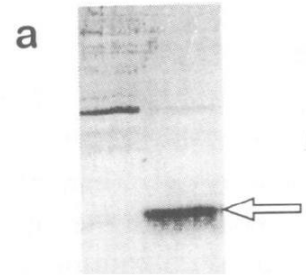
Early structural models proposed direct cation:π Interactions

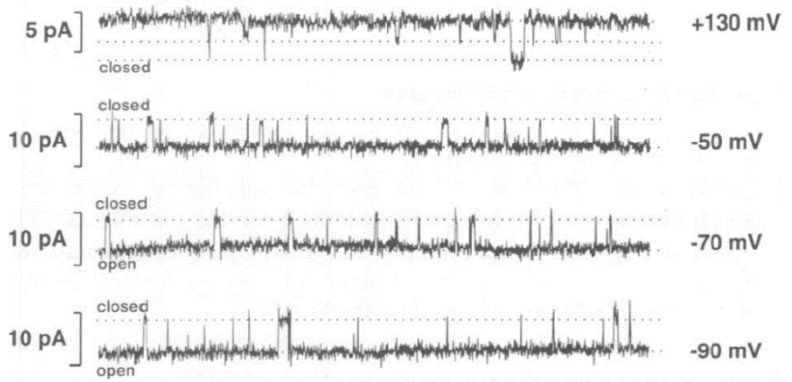
The EMBO Journal vol.14 no.21 pp.5170–5178, 1995

A prokaryotic potassium ion channel with two predicted transmembrane segments from *Streptomyces lividans*

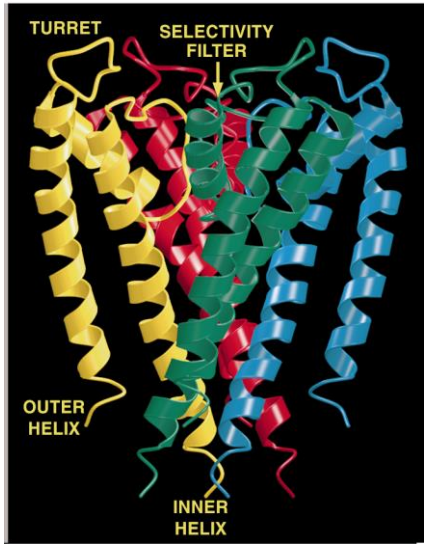
H.Schrempf[1], O.Schmidt, R.Kümmerlen, S.Hinnah[2], D.Müller, M.Betzler, T.Steinkamp[2] and R.Wagner[2]

Angewandte Genetik der Mikroorganismen and [2]Biophysik, FB Biologie/Chemie, Universität Osnabrück, 49069 Osnabrück, Germany









Problem Set

C7- MT7.2
Sensing and sensory cells

Sonia Contera

sonia.antoranzcontera@physics.ox.ac.uk

Reference:
Primary Processes in sensory cells
Stephan Frings, J Comp Physiol A (2009) 195:1-19

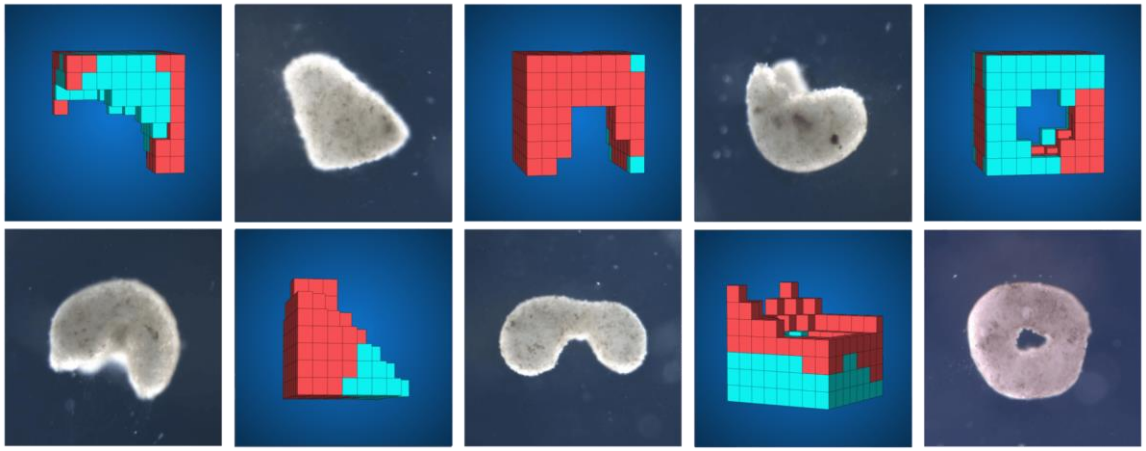
Transduction cascade

Primary signals have to be amplified and an out-put signal must be generated

- photoreceptors that detect single-photons
- mechanoreceptors that respond to the movements on a nanometer scale and
- chemoreceptors that report the detection of single molecules.

transduction mechanisms that mediate the analysis of **infrared radiation, electrical fields or magnetic navigation**

common transduction features begin to appear, new experimental approaches become available

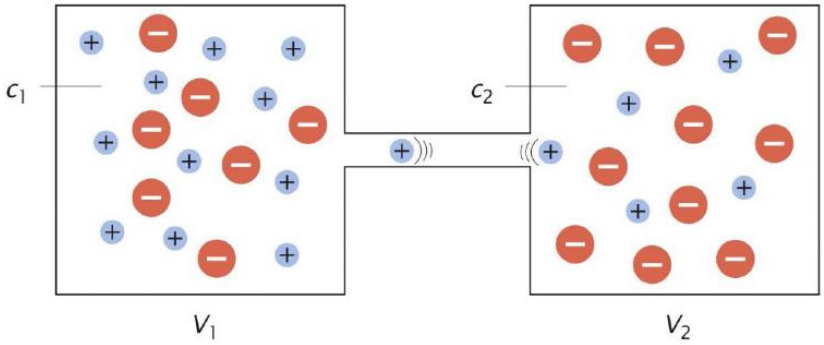


Living robots, "xenobots"

The Nernst equation

A simplified situation that illustrates the energetic and entropic competition which plays out when there are concentration gradients

1. Chemical free energy $\Delta G_{chemical} = kT ln \frac{c_1}{c_2}$
2. Electrical free energy $\Delta G_{electrical} = zeV_2 - V_1$



- Entropy grows
- Charge imbalance, i.e. an increase in electric energy
- Until equilibrium is reached

Electrostatic energy of a unit charge e when placed inside of a cell with potential V_{in}

$U = zeV_{in}$

If ions are separated into two regions with corresponding potentials V_{in} *and* V_{out}

$$\frac{c_1}{c_2} = \frac{e^{-zeV_1/kT}}{e^{-zeV_2/kT}}$$

$$V_2 - V_1 = \frac{kT}{ze} \ln \frac{c_1}{c_2} \quad \text{(Nernst Potential)} \qquad \frac{kT}{e} = 25 \text{ mV}$$

Nernst equation says that , in equilibrium, the electrochemical potential of any permeant ion species must be the same.

The voltage across neurons and other excitable cells is **10-100mV**..

A Simple Two–State Model Can Describe Many of the Features of Voltage Gating of Ion Channels

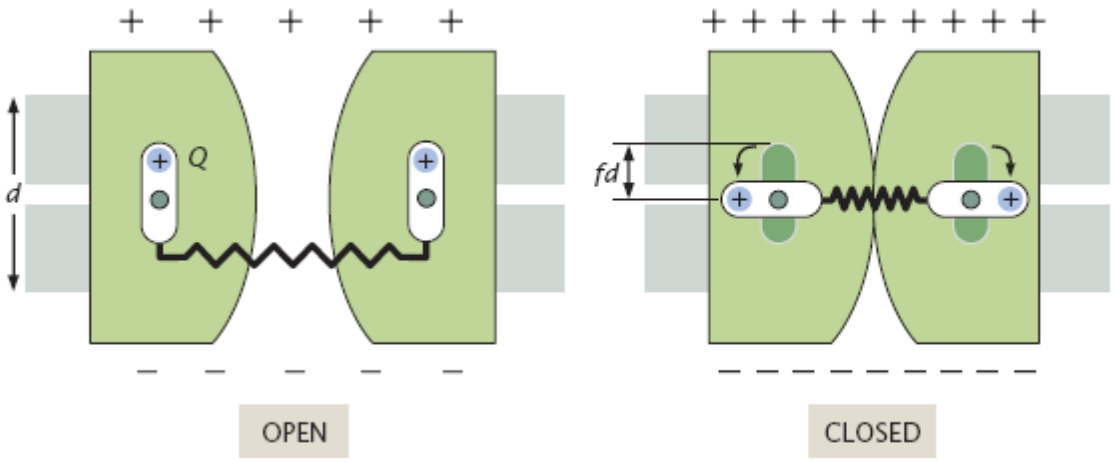


Figure 17.6: Two-state model of ion-channel voltage gating. In the open state, the "spring", representing the conformational degrees of freedom of the channel, is in the relaxed state and the gating charge, associated with the voltage-sensor part of the channel, is in the energetically costly state. In the closed state, the spring is in a compressed, high-energy state, but the gating charge has shifted favorably, by a fraction f of the membrane thickness d, with respect to the applied field. Note that we assume the total gating charge (the sum of the charges at both ends of the spring) to be Q.

competition between the

- *protein conformational degrees of freedom, represented in the toy model by a nonlinear spring,*
- *and the gating charge, which has an interaction energy with the applied field imposed by the membrane potential.*
- *Qualitatively, when the channel is open, the protein has lower energy (the spring is in the undeformed state) and the energy of the charge is higher than it would be in the closed state. When the channel is closed, the electric energy dominates and the protein energy is less favourable (that is, the spring is deformed).*

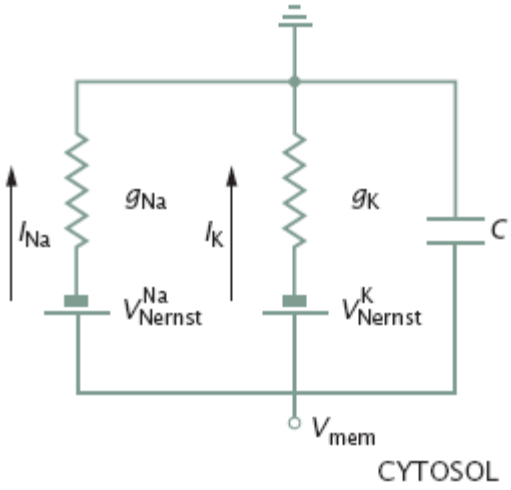


Figure 17.11: Mapping of a membrane onto an equivalent electrical circuit. The lipid bilayer yields the behavior of a capacitor of capacitance C, while the presence of channels can be modeled as resistors whose conductances (inverse resistances) are g_{Na} and g_K for the sodium and potassium channels, respectively. The batteries represent the Nernst potentials for each of the individual ionic species, which account for the ionic currents due to the concentration gradient across the membrane.

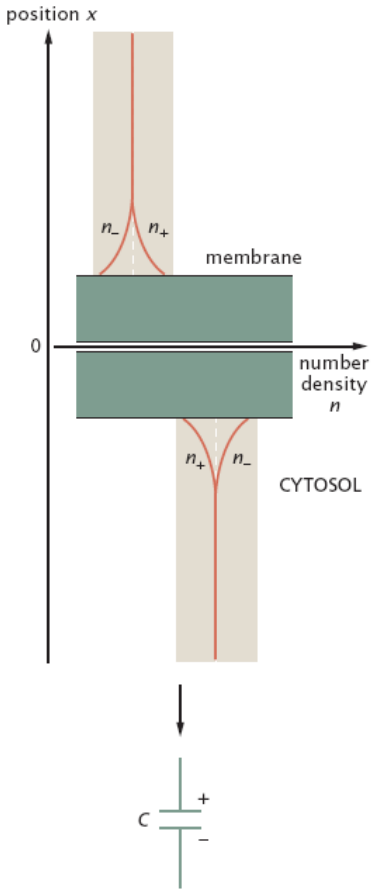
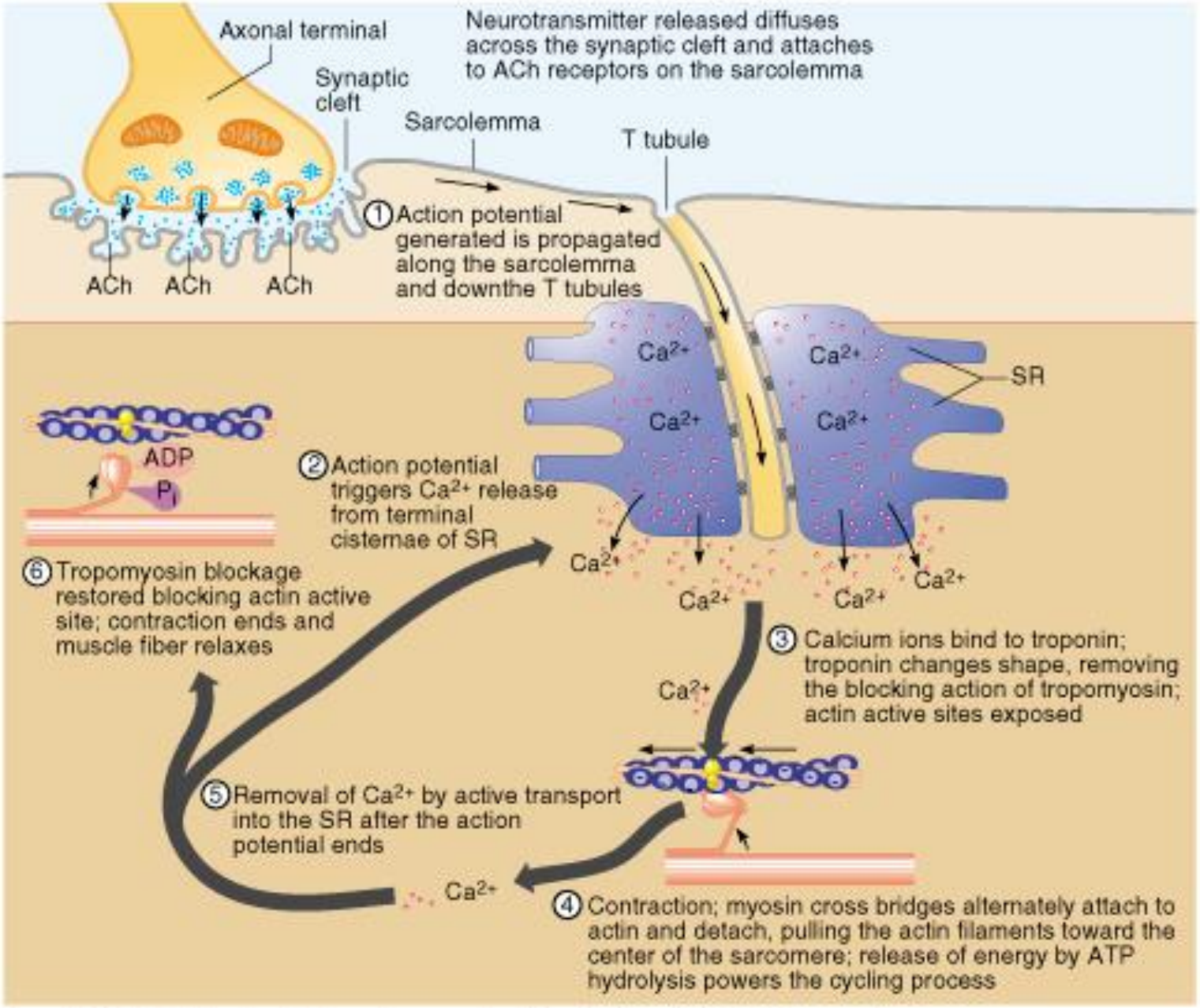


Figure 17.12: Membrane capacitance. There is an excess negative charge inside the cell (cytosol side) and an excess positive charge on the outside, leading to a voltage drop across the membrane, just like in a parallel-plate capacitor. The charge imbalance is present in a thin layer next to the cell membrane, whose width is of the order of the Debye length. The net charge at the surface of the membrane and the membrane voltage are related to each other by the membrane capacitance $C = Q/V_{mem}$.



Copyright © 2001 Benjamin Cummings, an imprint of Addison Wesley Longman, Inc.

Touch

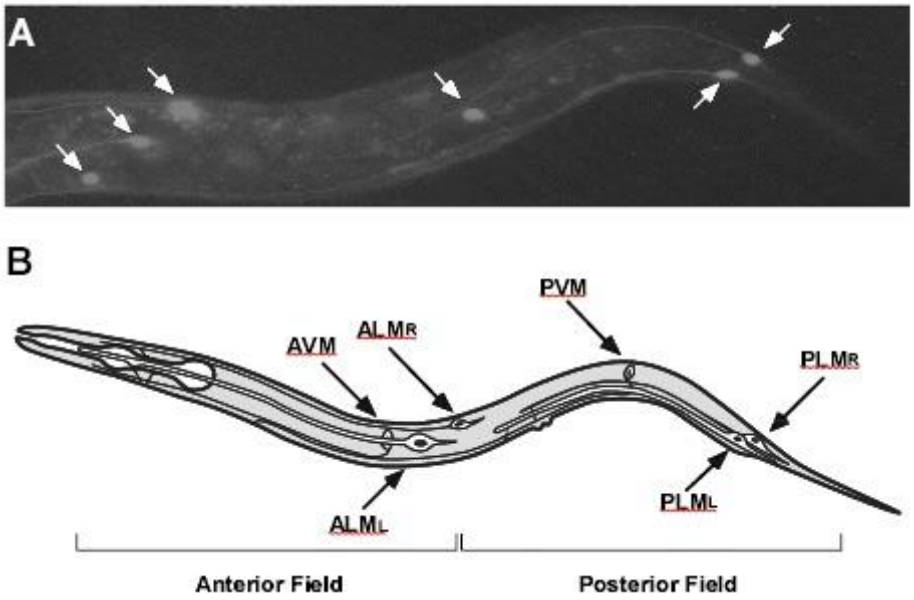


Figure 1
The two fields of touch sensitivity are defined by the arrangement of touch receptor neurons along the body axis. The ALMs and AVM mediate the response to touch over the anterior field whereas PLMs mediate the response to touch over the posterior field. PVM does not mediate touch response by itself
From: Mechanotransduction in the Nematode *Caenorhabditis elegans*

Mechanosensitivity in Cells and Tissues.
Kamkin A, Kiseleva I, editors.
Moscow: Academia; 2005.
Copyright © 2005, Academia Publishing House Ltd.
NCBI Bookshelf. A service of the National Library of Medicine, National Institutes of Health.

this basic and omni- present sense appears to be one of the most difficult to study on the level of its transduction mechanism.

It is quite clear that mechanical stimuli of various sorts can trigger opening of ion channels and cause depolarization in practically every cell (Hamill and Martinac 2001; Kung 2005 ; Hamill 2006). However, **sensory cells which are specialized for the detection of mechanical stimuli (mechanoreceptors) can use elaborate protein complexes to transduce adequate mechanical stimuli, and to report a sensory signal to the central nervous system.** How intricate the structure of such a transducer can be revealed by an extensive genetic screening of Caenorhabditis elegans mutants which took more than 25 years and brought to light a set of proteins that co- assemble to form a mechanotransduction complex

- **O'Hagan and Chalfe 2006**
- **Bianchi 2007**
- **Bounoutas and Chalfe 2007**

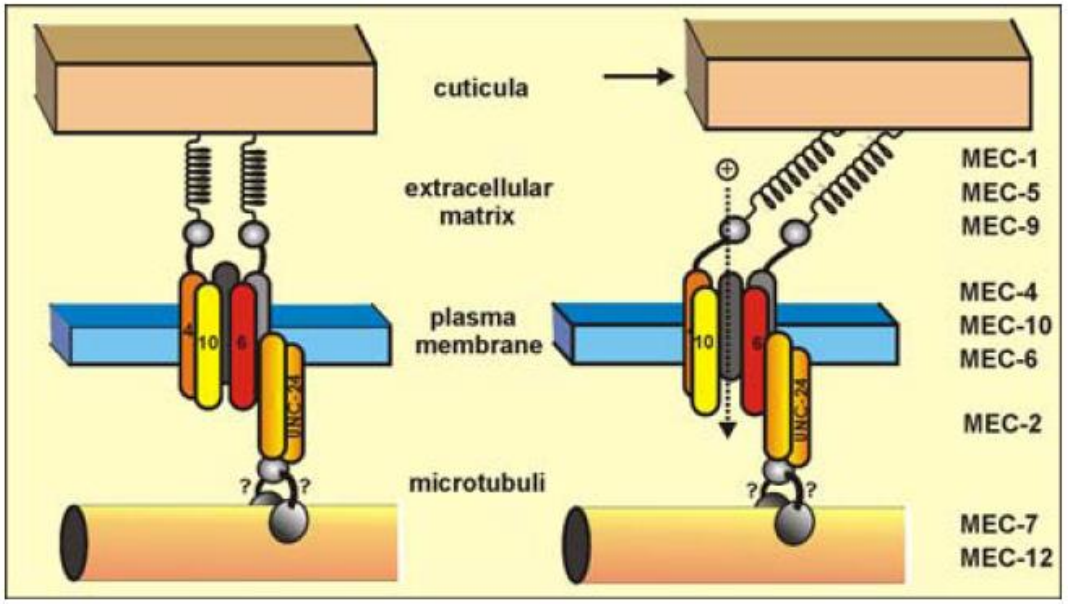
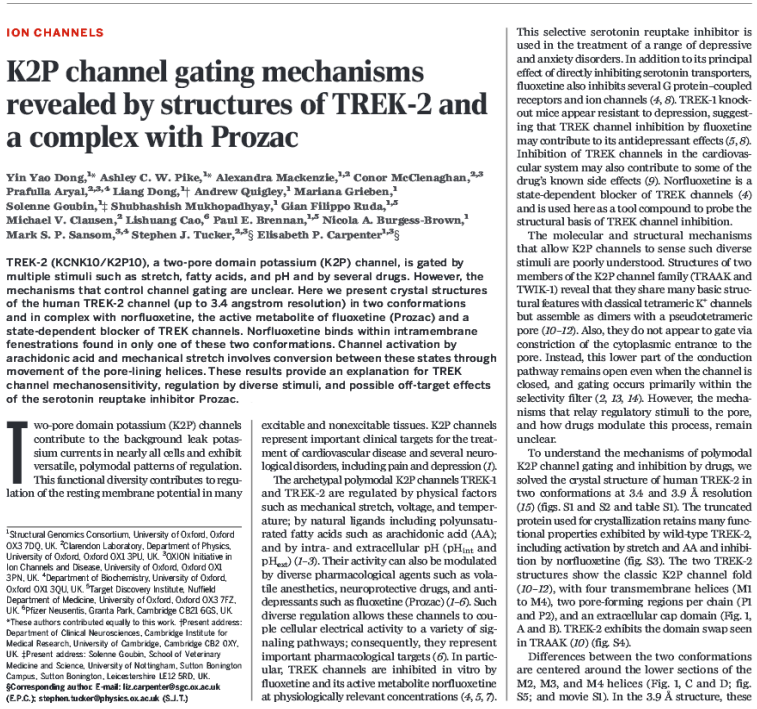


Fig. 1 The mechanosensitive protein complex of *C. elegans*. *Left:* nine different MEC proteins co-assemble to form an ion channel in the plasma membrane of a mechanosensory neuron. The channel is formed by MEC-4, MEC-6, and MEC-10. Other MEC proteins tether the channel to the cuticula and to the cytoskeleton. *Right:* when the cuticula is shifted by gentle touch, the channel is pulled open, and cation influx generates a receptor potential

A member of the PHB domain protein family, stomatin-like protein 3 (SLP3), turned out to be necessary for normal touch sensation in mice (Wetzel et al. 2007). The related protein stomatin is needed for sensory function in rapidly adapting D-hair mechanoreceptors (Martinez-Salgado et al. 2007). These findings suggest that SLP3 and stomatin play a similar role in vertebrate mechanotransduction as MEC-2 plays in the C. elegans touch receptor. Although it is too early to speculate the notion that vertebrate mechanotransducers are protein complexes with tethered transduction channels appears to be a reasonable working hypothesis. Future work may lead to the identification of multiple transduction components and to gene ablation experiments with unambiguous phenotypes. Up to now, the search for mechanotransduction channels has only produced conflicting results (Drew et al. 2004; Gottlieb et al. 2008), and the molecular identity of the channels remains elusive.



ION CHANNELS

K2P channel gating mechanisms revealed by structures of TREK-2 and a complex with Prozac

Yin Yao Dong,[1*] Ashley C. W. Pike,[1*] Alexandra Mackenzie,[1,2] Conor McClenaghan,[2,3] Prafulla Aryal,[2,3,4] Liang Dong,[1†] Andrew Quigley,[1] Mariana Grieben,[1] Solenne Goubin,[1‡] Shubhashish Mukhopadhyay,[1] Gian Filippo Ruda,[1,5] Michael V. Clausen,[2] Lishuang Cao,[6] Paul E. Brennan,[1,5] Nicola A. Burgess-Brown,[1] Mark S. P. Sansom,[2,4] Stephen J. Tucker,[2,3]§ Elisabeth P. Carpenter[1,3]§

TREK-2 (KCNK10/K2P10), a two-pore domain potassium (K2P) channel, is gated by multiple stimuli such as stretch, fatty acids, and pH and by several drugs. However, the mechanisms that control channel gating are unclear. Here we present crystal structures of the human TREK-2 channel (up to 3.4 angstrom resolution) in two conformations and in complex with norfluoxetine, the active metabolite of fluoxetine (Prozac) and a state-dependent blocker of TREK channels. Norfluoxetine binds within intramembrane fenestrations found in only one of these two conformations. Channel activation by arachidonic acid and mechanical stretch involves conversion between these states through movement of the pore-lining helices. These results provide an explanation for TREK channel mechanosensitivity, regulation by diverse stimuli, and possible off-target effects of the serotonin reuptake inhibitor Prozac.

Two-pore domain potassium (K2P) channels contribute to the background leak potassium currents in nearly all cells and exhibit versatile, polymodal patterns of regulation. This functional diversity contributes to regulation of the resting membrane potential in many excitable and nonexcitable tissues. K2P channels represent important clinical targets for the treatment of cardiovascular disease and several neurological disorders, including pain and depression (*1*).

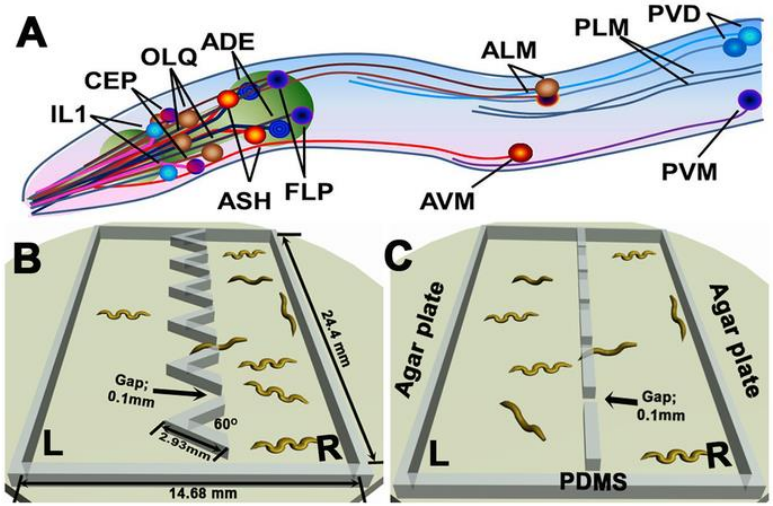
The archetypal polymodal K2P channels TREK-1 and TREK-2 are regulated by physical factors such as mechanical stretch, voltage, and temperature; by natural ligands including polyunsaturated fatty acids such as arachidonic acid (AA); and by intra- and extracellular pH (pH_{int} and pH_{ext}) (*1–3*). Their activity can also be modulated by diverse pharmacological agents such as volatile anesthetics, neuroprotective drugs, and antidepressants such as fluoxetine (Prozac) (*1–6*). Such diverse regulation allows these channels to couple cellular electrical activity to a variety of signaling pathways; consequently, they represent important pharmacological targets (*6*). In particular, TREK channels are inhibited in vitro by fluoxetine and its active metabolite norfluoxetine at physiologically relevant concentrations (*4, 5, 7*). This selective serotonin reuptake inhibitor is used in the treatment of a range of depressive and anxiety disorders. In addition to its principal effect of directly inhibiting serotonin transporters, fluoxetine also inhibits several G protein–coupled receptors and ion channels (*4, 8*). TREK-1 knockout mice appear resistant to depression, suggesting that TREK channel inhibition by fluoxetine may contribute to its antidepressant effects (*5, 8*). Inhibition of TREK channels in the cardiovascular system may also contribute to some of the drug's known side effects (*9*). Norfluoxetine is a state-dependent blocker of TREK channels (*4*) and is used here as a tool compound to probe the structural basis of TREK channel inhibition.

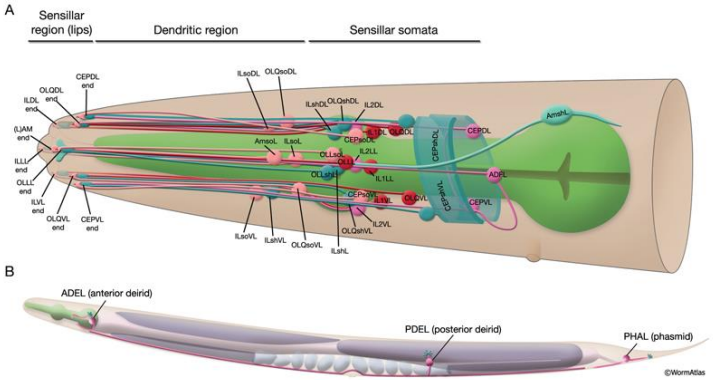
The molecular and structural mechanisms that allow K2P channels to sense such diverse stimuli are poorly understood. Structures of two members of the K2P channel family (TRAAK and TWIK-1) reveal that they share many basic structural features with classical tetrameric K^+ channels but assemble as dimers with a pseudotetrameric pore (*10–12*). Also, they do not appear to gate via constriction of the cytoplasmic entrance to the pore. Instead, this lower part of the conduction pathway remains open even when the channel is closed, and gating occurs primarily within the selectivity filter (*2, 13, 14*). However, the mechanisms that relay regulatory stimuli to the pore, and how drugs modulate this process, remain unclear.

To understand the mechanisms of polymodal K2P channel gating and inhibition by drugs, we solved the crystal structure of human TREK-2 in two conformations at 3.4 and 3.9 Å resolution (*15*) (figs. S1 and S2 and table S1). The truncated protein used for crystallization retains many functional properties exhibited by wild-type TREK-2, including activation by stretch and AA and inhibition by norfluoxetine (fig. S3). The two TREK-2 structures show the classic K2P channel fold (*10–12*), with four transmembrane helices (M1 to M4), two pore-forming regions per chain (P1 and P2), and an extracellular cap domain (Fig. 1, A and B). TREK-2 exhibits the domain swap seen in TRAAK (*10*) (fig. S4).

Differences between the two conformations are centered around the lower sections of the M2, M3, and M4 helices (Fig. 1, C and D; fig. S5; and movie S1). In the 3.9 Å structure, these

[1]Structural Genomics Consortium, University of Oxford, Oxford OX3 7DQ, UK. [2]Clarendon Laboratory, Department of Physics, University of Oxford, Oxford OX1 3PU, UK. [3]OXION Initiative in Ion Channels and Disease, University of Oxford, Oxford OX1 3PN, UK. [4]Department of Biochemistry, University of Oxford, Oxford OX1 3QU, UK. [5]Target Discovery Institute, Nuffield Department of Medicine, University of Oxford, Oxford OX3 7FZ, UK. [6]Pfizer Neusentis, Granta Park, Cambridge CB21 6GS, UK. *These authors contributed equally to this work. †Present address: Department of Clinical Neurosciences, Cambridge Institute for Medical Research, University of Cambridge, Cambridge CB2 0XY, UK. ‡Present address: Solenne Goubin, School of Veterinary Medicine and Science, University of Nottingham, Sutton Bonington Campus, Sutton Bonington, Leicestershire LE12 5RD, UK. §Corresponding author. E-mail: liz.carpenter@sgc.ox.ac.uk (E.P.C.); stephen.tucker@physics.ox.ac.uk (S.J.T.)





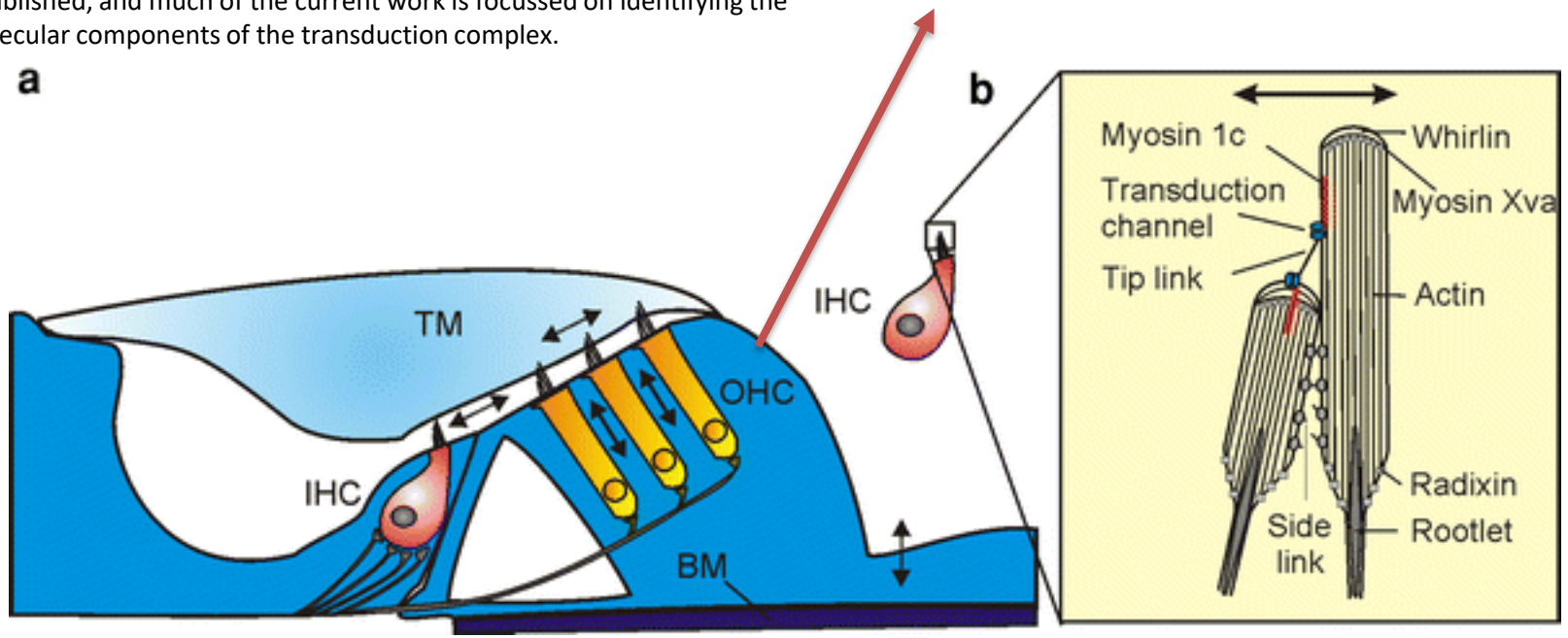
It is conceivable, although entirely speculative, that the detection of gentle touch **relies on multi-protein transduction** complexes in vertebrate touch receptor neurons, while nociceptors respond to their much stronger stimuli with **simple stretch-sensitive channels**. It is also possible that the *C. elegans*-type transduction complex and the stretch-sensitive channel do not represent mutually exclusive gating principles. There may be various intermediate structures with transduction channels attached to the cytoskeleton or to proteins in the membrane or the extracellular matrix.

Hearing

The tethered-channel hypothesis is now well established

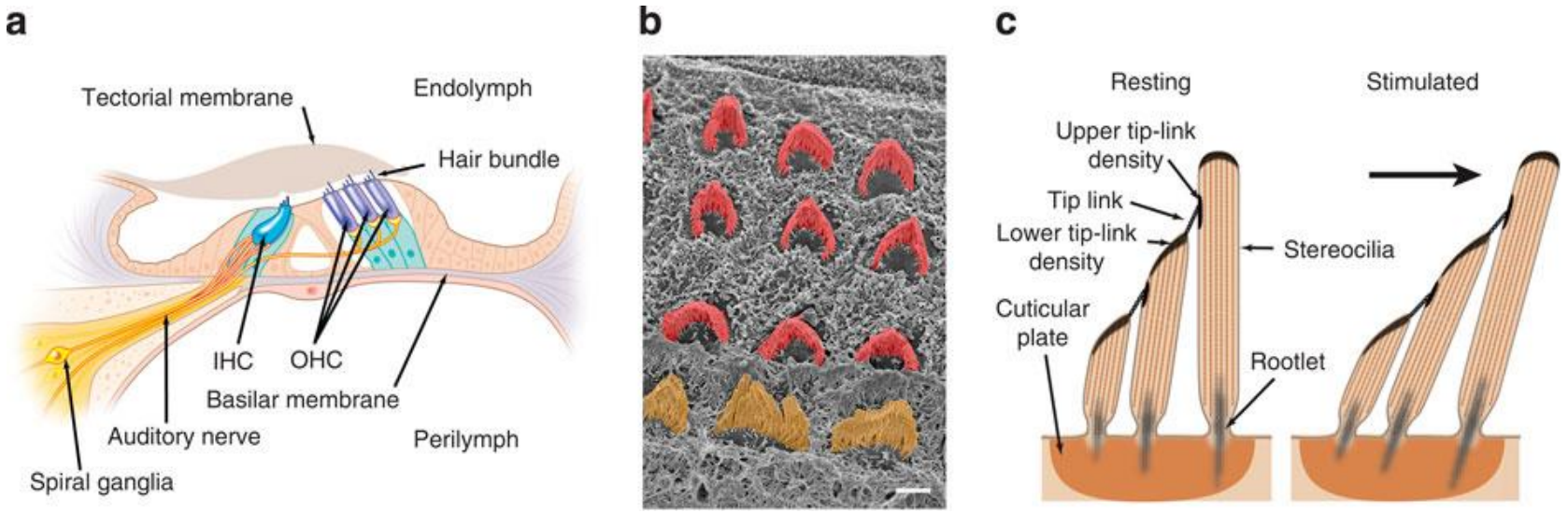
A fascinating example of vertebrate mechanosensory transduction by tethered channels is the generation of receptor potentials in the **hair cells of the inner ear. These exquisitely sensitive cells detect movements on a nanometer scale** by their apical hair bundles and transmit the sensory signal to afferent neurons with high efficiency. **Based on groundbreaking electrophysiological studies (Corey and Hudspeth 1979; Hudspeth 1982; Corey and Hudspeth 1983) and the discovery of protein filaments connecting the sterocilia within a hair bundle (Pickles et al. 1984; Furness and Hackney 1985), a working hypothesis was formulated that explained hair-cell function in terms of a tethered transduction channel (Pickles 1985; Holton and Hudspeth 1986; Hudspeth 1989)**. An impressive array of excellent biophysical investigations was since carried out to scrutinize and improve this hypothesis (recent reviews: Gillespie et al. 2005; Corey 2006; Fettiplace and Hackney 2006; Ricci et al. 2006; Grant and Fuchs 2007; Vollrath et al. 2007). Today, the tethered-channel hypothesis is well established, and much of the current work is focussed on identifying the molecular components of the transduction complex.

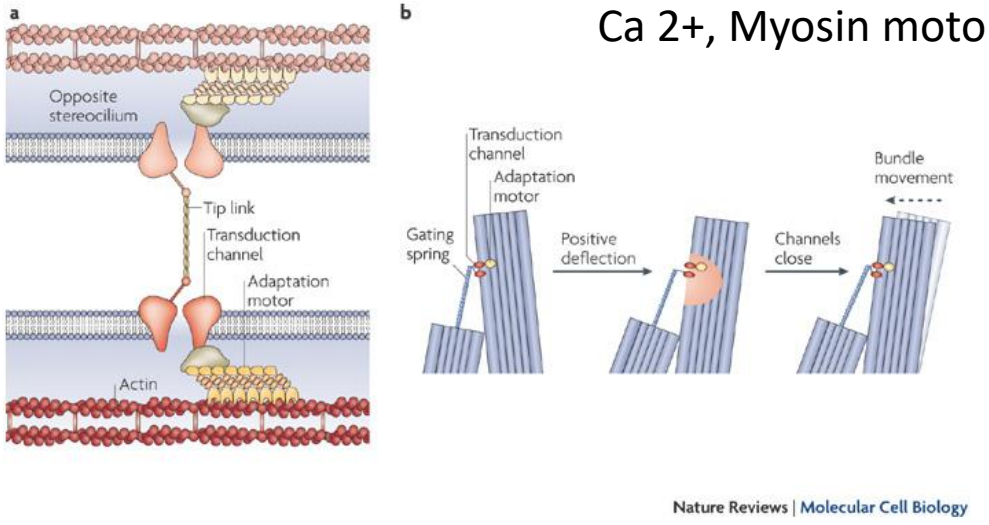
OHS electromotility to amplify 100-1000x
Contract upon depolarization/elongate hyperpolarization (PIEZO)
(10 ^-16 W/cm^2)



Hair cells in the organ of Corti. **a** Schematical cross-section of the organ of Corti with the tectorial membrane (TM) covering the stereocilia of sensory inner hair cells (IHC) and electromotile outer hair cells (OHC). **Sound induces local vibrations of the basilar membrane (BM) and a lateral displacement of hair-cell stereocilia (*arrows*)**. **b** Enlarged view of the stereocilia of an inner hair cell. **The transduction channels of the longer stereocilium are dynamically anchored to actin filaments through myosin 1c. A tip-link filament pulls the transduction channels open when the stereocilia move in the plane indicated by the arrow**

tethered-channels





Ca 2+, Myosin motors keep the tension.

Neurosensory mechanotransduction
Martin Chalfie
Nature Reviews Molecular Cell Biology 10, 44-52 (January 2009)

Phototransduction: dynamic scaffolds

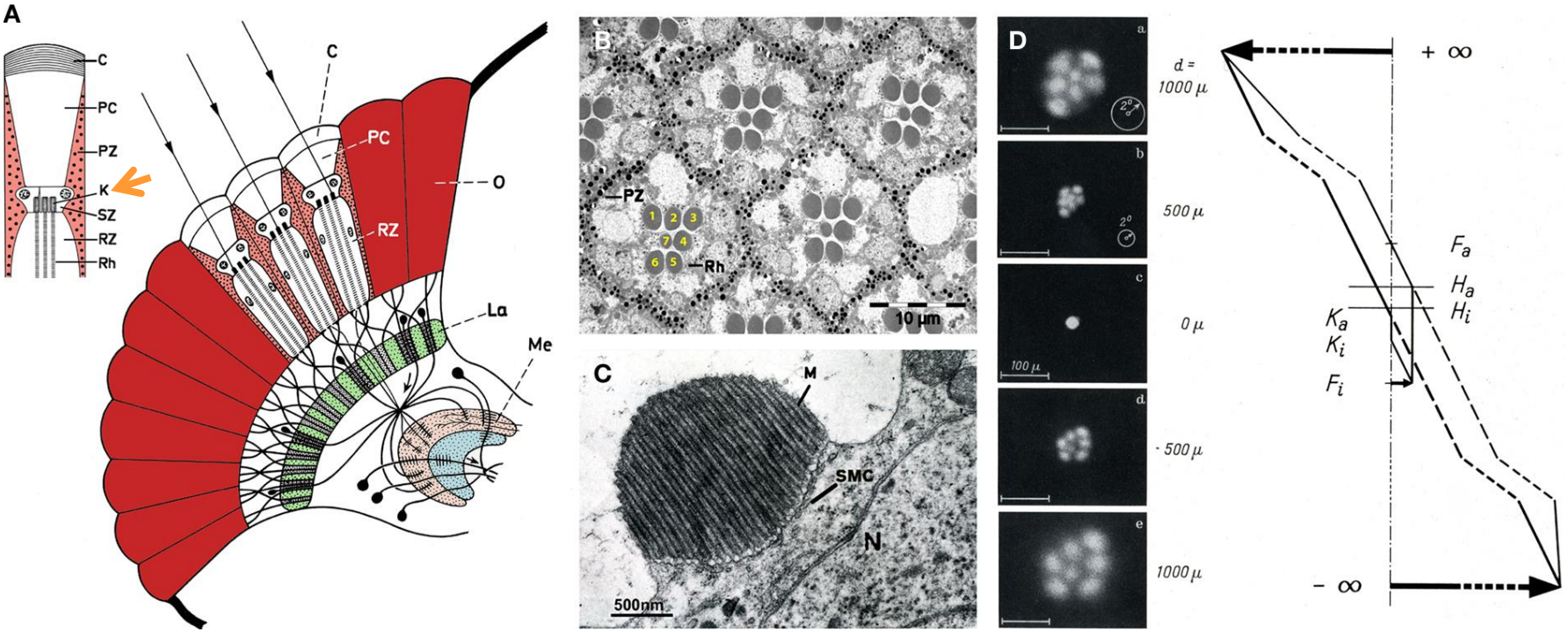
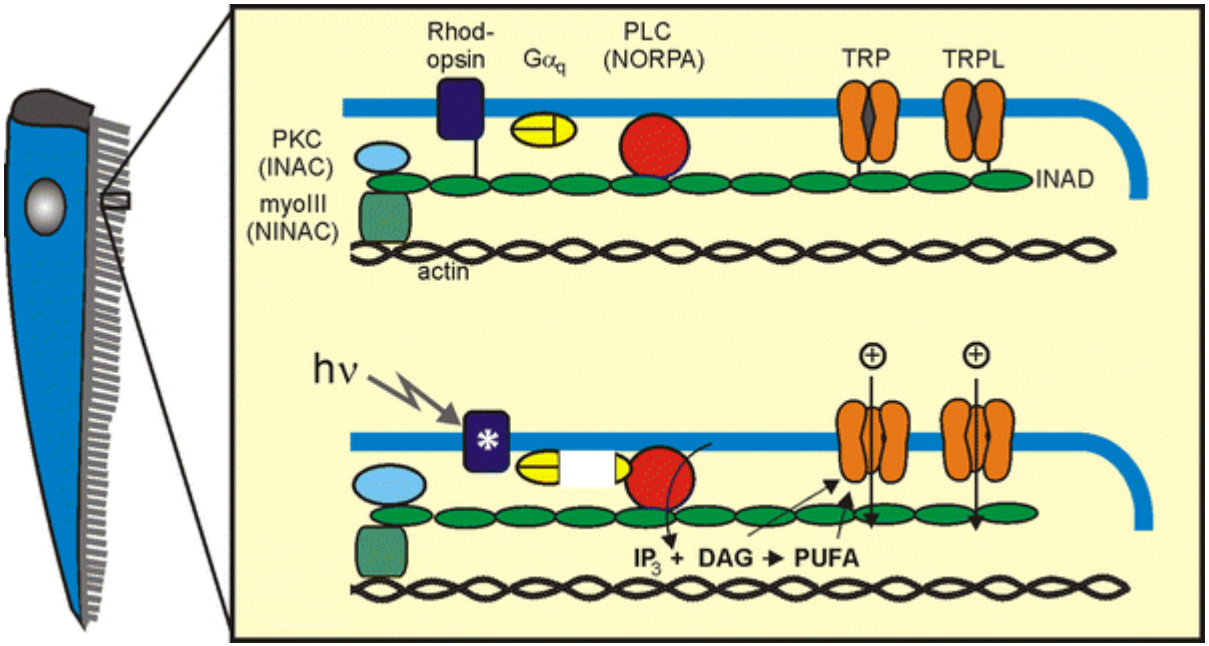


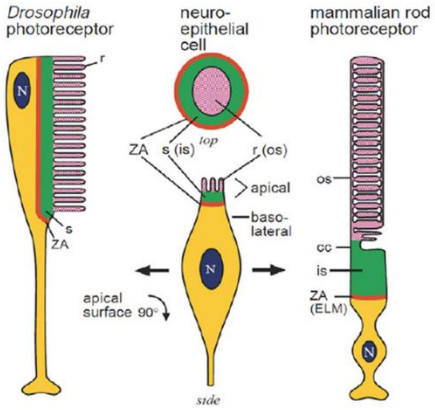
Figure 1. The morphology and optics of the compound eye. (A) The compound eye of *Musca* and **the visual ganglionic layers:** a schematic representation of a horizontal section. Inset – Schematic representation of the distal area of a single ommatidium. **C – corneal lens, PC – pseudocone**, RZ – retinula cells (photoreceptor), PZ – pigment cells, **K – rhabdomere** cap, SZ – Semper cells, Rh – rhabdomere, La – lamina, Me – medulla (modified from Kirschfeld, 1967). **(B,C)** Electron microscopic (EM) cross-section of *Drosophila* ommatidia and a **rhabdomere at the upper region of the photoreceptors respectively**. **M – microvilli**, SMC – submicrovillar cisternae, N – nucleus (modified from Minke and Selinger, 1996). **(D)** Optical properties of a single ommatidium demonstrated by "antidromic" illumination in *Musca* when a 30 µm diaphragm is placed over a single ommatidium seen when focused at the cornea (0 µm). Inverted images of the rhabdomere tips are seen when focusing above the cornea (1000 µm and 500 µm) and upright images below the cornea (−500 µm and −1000 µm). The optical path is shown on the right, F – focal plane, H – main plane, K – junction, a – outer, i – inner (modified from Kirschfeld and Franceschini, 1968).

Light dependent restructuring



The signalplex of fly photoreceptors. Schematical view of primary processes in a **microvillus from a fly rhabdomer**. A polymer of INAD scaffold proteins coordinates the transduction proteins rhodopsin, $G\alpha_q$, phospholipase C (PLC), protein kinase C (PKC), transient receptor potential channel (TRP), and TRP-like channel (TRPL). Illumination leads to release of inositol-1,4,5-trisphosphate (IP_3), diacylglycerol (DAG), and polyunsaturated fatty acids (PUFA), which open the TRP/TRPL channels

GARP scaffold protein in vertebrates



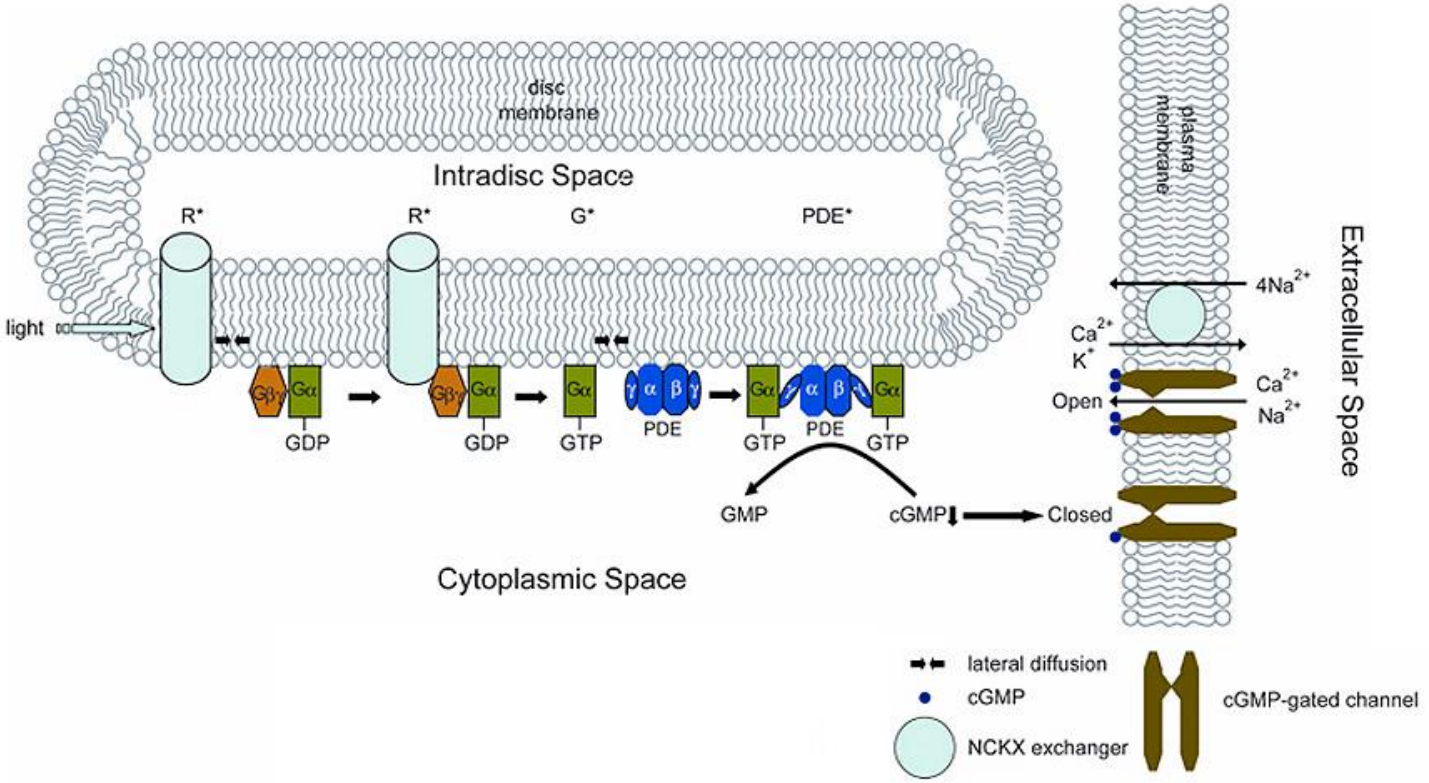
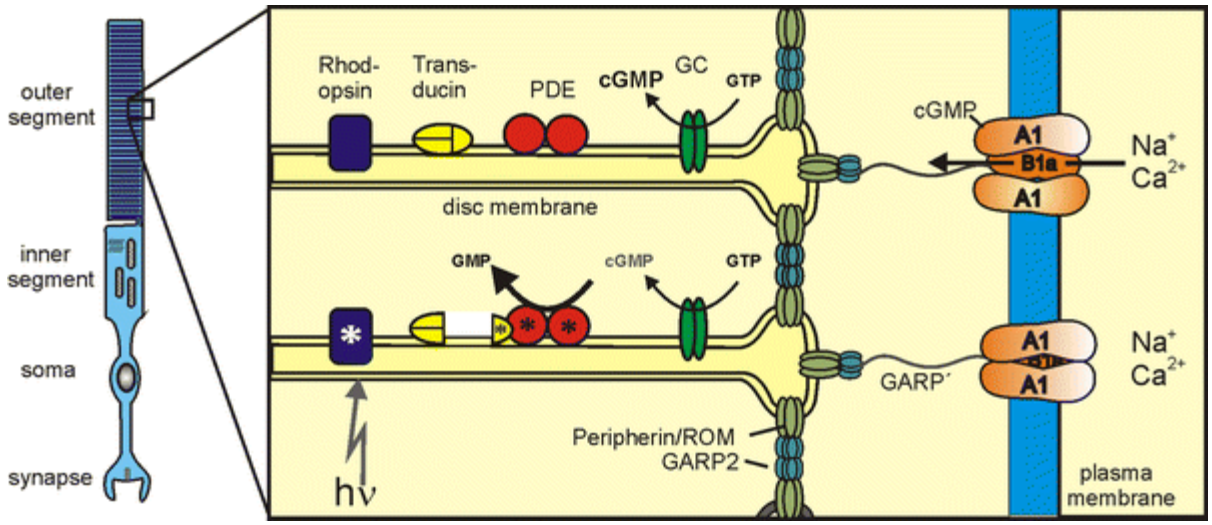
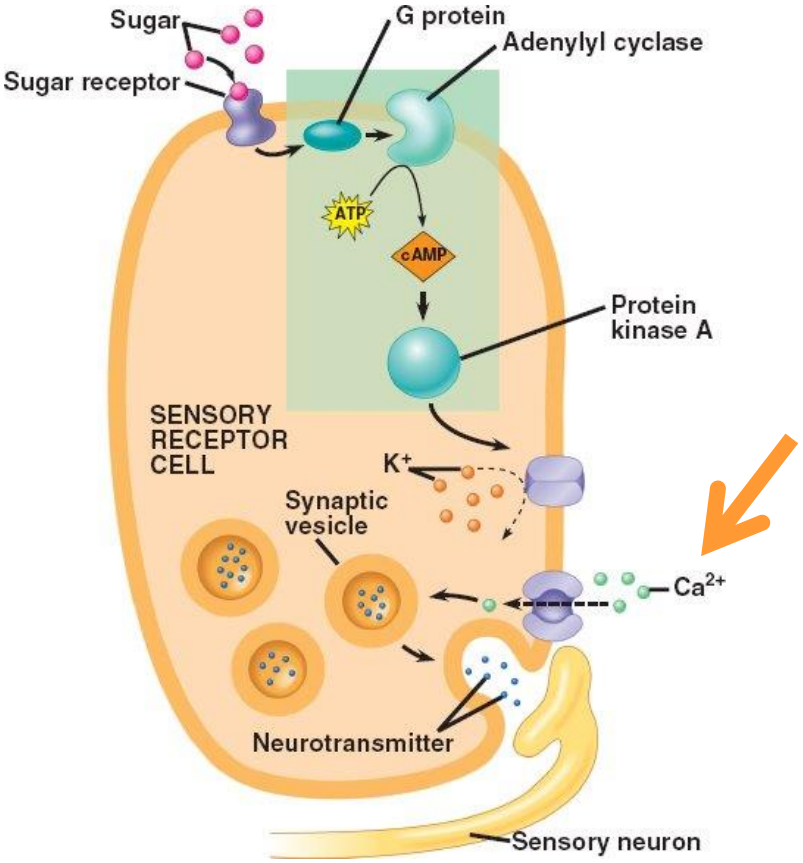


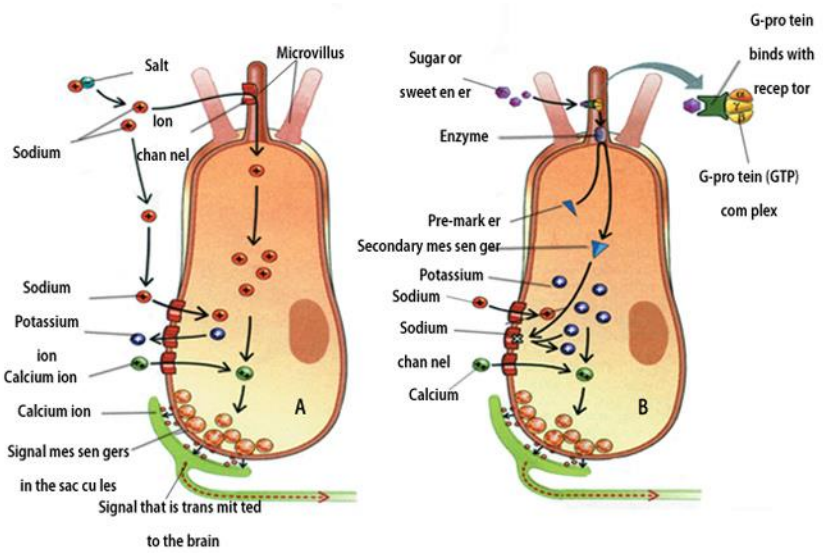
Figure 7. Schematic representation on the activation of vertebrate rod phototransduction. Following photon absorption, the activated rhodopsin (R*) activates the heterotrimeric G protein, catalyzing the exchange of GDP for GTP, producing the active Gα*-GTP. Two Gα*-GTP bind to the two inhibitory γ subunits of PDE, thereby releasing the inhibition on the catalytic α and β subunits, forming PDE*, which in turn catalyzes the hydrolysis of cGMP. The consequent decrease in the cytoplasmic free cGMP concentration leads to the closure of the cGMP-gated channels on the plasma membrane and blockage of the influx of cations into the outer segment, which results in the reduction of the circulating dark current.



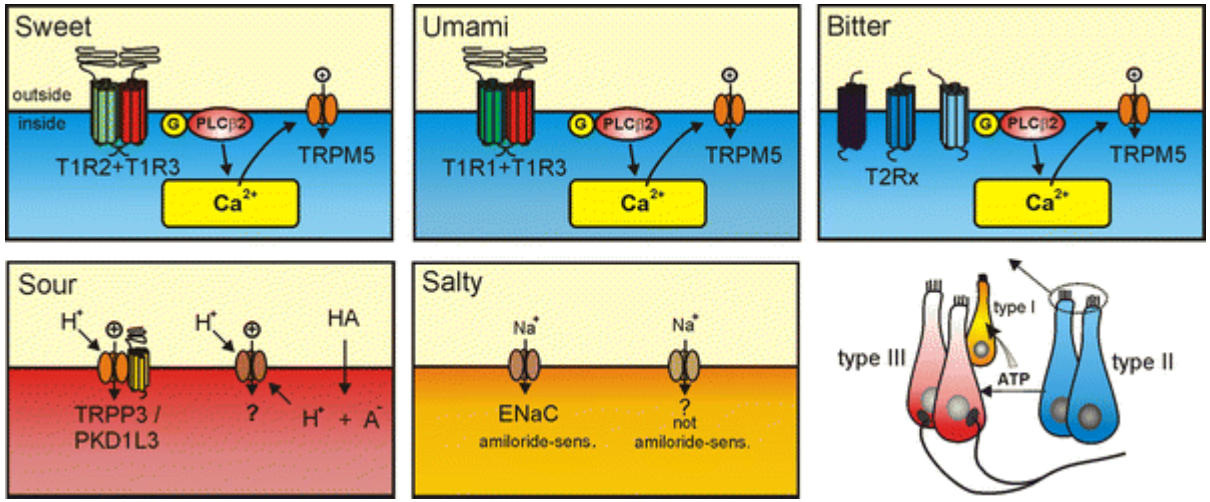
The rim region of the vertebrate photoreceptor outer segment. cGMP-gated transduction channels in the plasma membrane (with their subunits CNGA1 and CNGB1a) are connected to the intracellular disc membrane via **a GARP' domain** (GARP, glutamic acid-rich protein) which forms the C-terminus of each CNGB1a subunit. **Soluble GARP and peripherin connect discs and transduction channels in the rim region**. *cGMP* cyclic guanosine monophosphate, *GC* guanylyl cyclase, *GTP* guanosine triphosphate, *PDE* phosphodiesterase, *ROM* rod outer segment membrane protein.
Illumination leads to a decline of the cGMP concentration and closure of cGMP-gated cation channels

Taste system





Taste transduction: gustatory genetics



Primary processes in taste cells. Transduction models for the chemosensory membrane of taste cells. The metabotropic receptor families T1R and T2R mediate sensitivity to sweet, umami, and bitter by activating phospholipase β2 (PLCβ2) **through a GTP-binding protein** (G). The resulting release of Ca2+ from intracellular stores **opens transient receptor potential M5 channels** (TRPM5) which generate a depolarizing receptor potential. Sour taste is mediated by a combination of transient receptor potential P3 channels (TRPP3) and polycystic-kidney-desease-like ion channels (PKD1L3). **Additional pH effects on other ion channels, as well as proton uptake into taste cells have also been reported.** Salt taste may, in part, be mediated by **Na+-permeable epithelial sodium channels (ENaC). Sweet, umami, and bitter taste resides in type II cells (blue) which release ATP as paracrine transmitter**. Sour taste is located in the presynaptic type III cells (red), and salt taste is mediated by type I cells (yellow) which also remove ATP from the taste bud

ANDREW SWIFT FOR THE SCIENTIST, NOVEMBER 2011

TASTE IN THE GUT

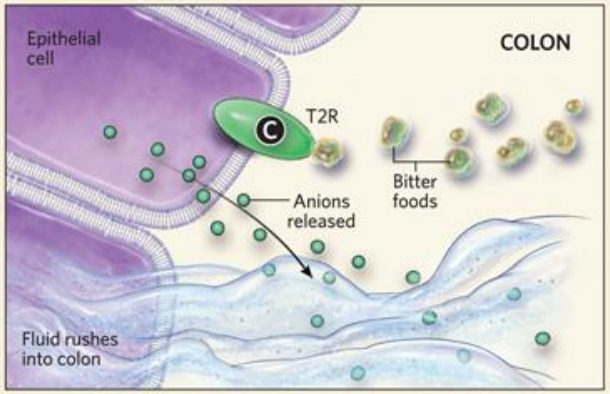
In contrast to taste receptors in the mouth, T1R and T2R receptors in the gut do not induce sensations of taste, but rather initiate molecular pathways that help guide the digestion or rejection of food substances traveling through the intestines. The underlying pathways, however, have many similarities.

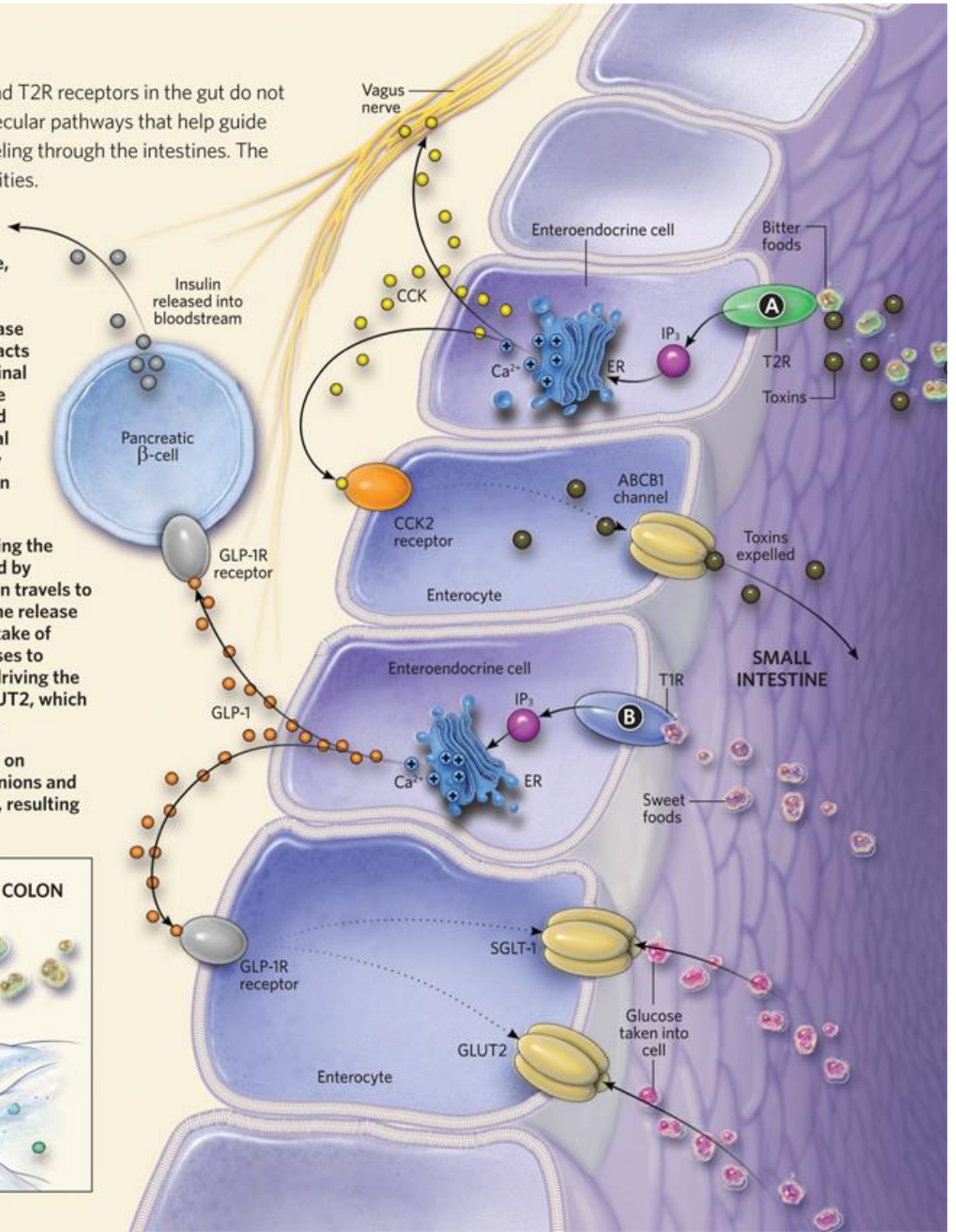
FOODS IN THE GUT

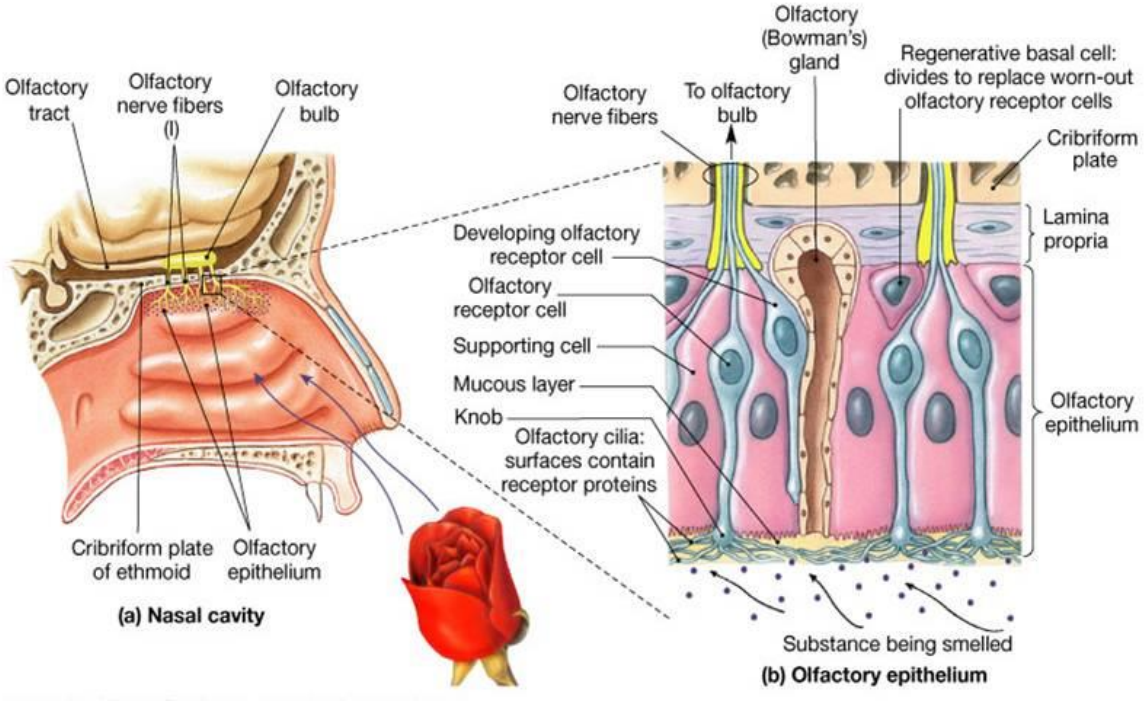
A **Specialized endocrine cells of the small intestine, known as enteroendocrine cells, display T2R bitter receptors on their cell membranes. When bitter compounds bind to the T2R receptors, the cells release the peptide hormone cholecystokinin (CCK), which acts on CCK2 receptors located on enterocytes, or intestinal absorptive cells. This increases the expression of the transporter ABCB1, which pumps toxins or unwanted substances out of the cell and back into the intestinal lumen. CCK also binds to CCK1 receptors on sensory fibers of the vagus nerve, sending signals to the brain to cease food intake.**

B **T1R-class receptors on enteroendocrine cells lining the small intestine detect sweet substances and respond by secreting the glucagon-like peptide GLP-1. GLP-1 then travels to the pancreas via the bloodstream, where it boosts the release of insulin from pancreatic β-cells, promoting the uptake of glucose by diverse tissues. Additionally, GLP-1 diffuses to neighboring enterocyte cells in the small intestine, driving the insertion of the glucose transporters SGLT-1 and GLUT2, which facilitates the uptake of glucose from the intestines.**

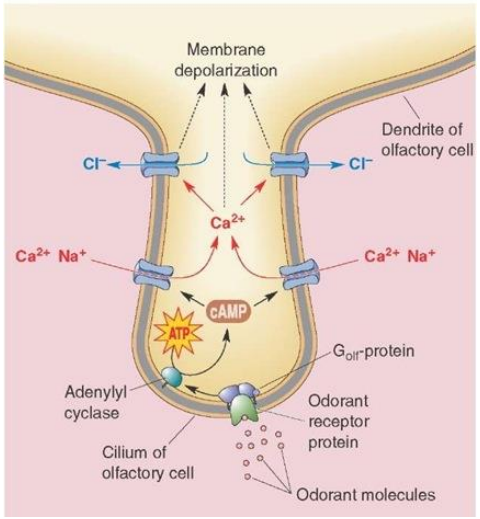
C **In the colon, bitter ligands bind to T2R receptors on epithelial cells, where they induce the secretion of anions and water, which leads to fluid rushing into the intestine, resulting in diarrhea that flushes out the colon.**

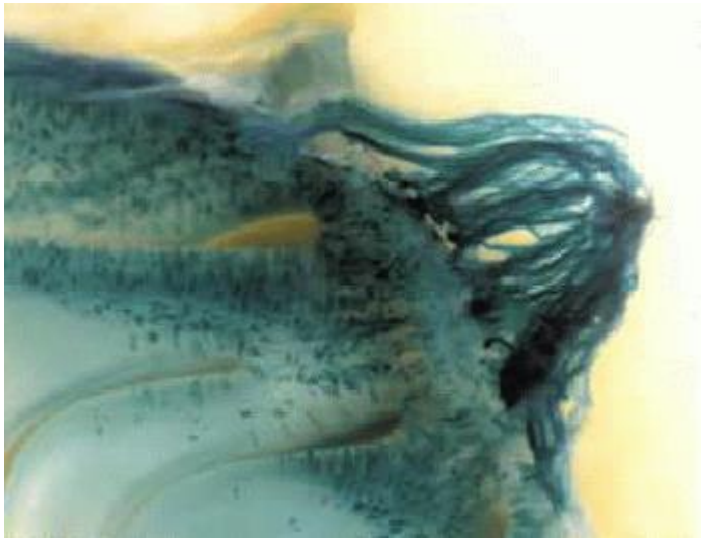


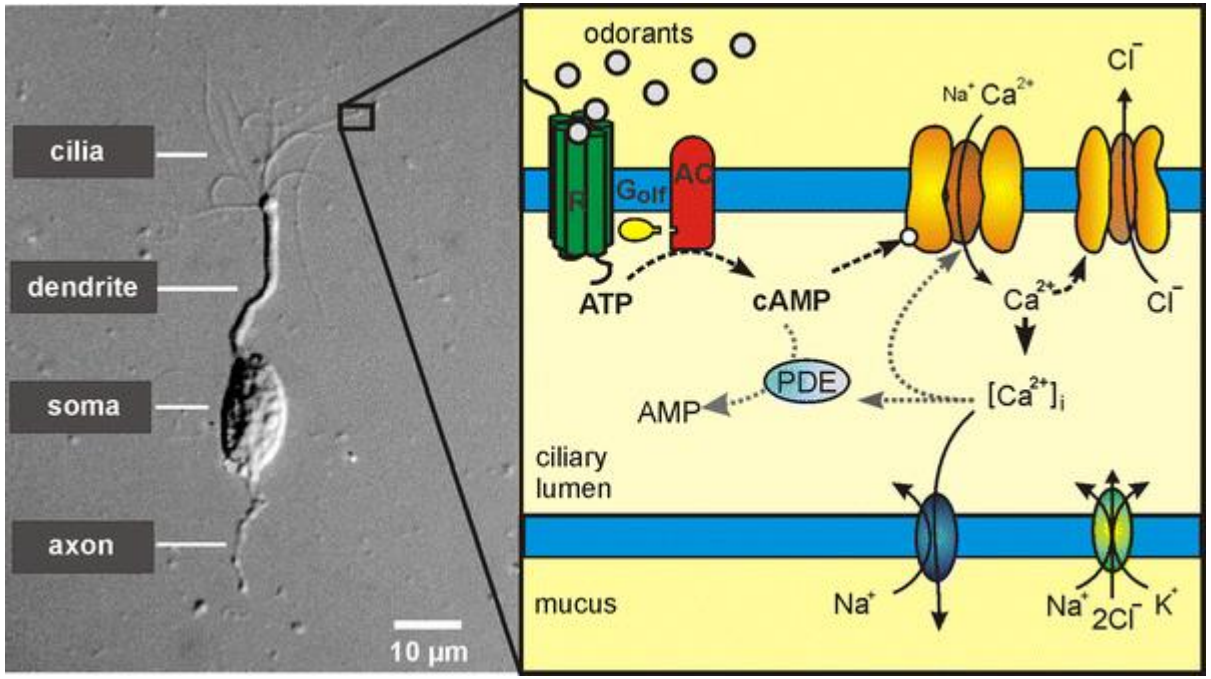




- **Only a single olfactory receptor gene is expressed in each individual ORN (olfactory receptor neurons)**
- **1,000 receptors each can bind different odorants**
- **1ms mean dwell time**
- **Mucus layer of odorant binding proteins, can shuttle hydrophobic molecules**

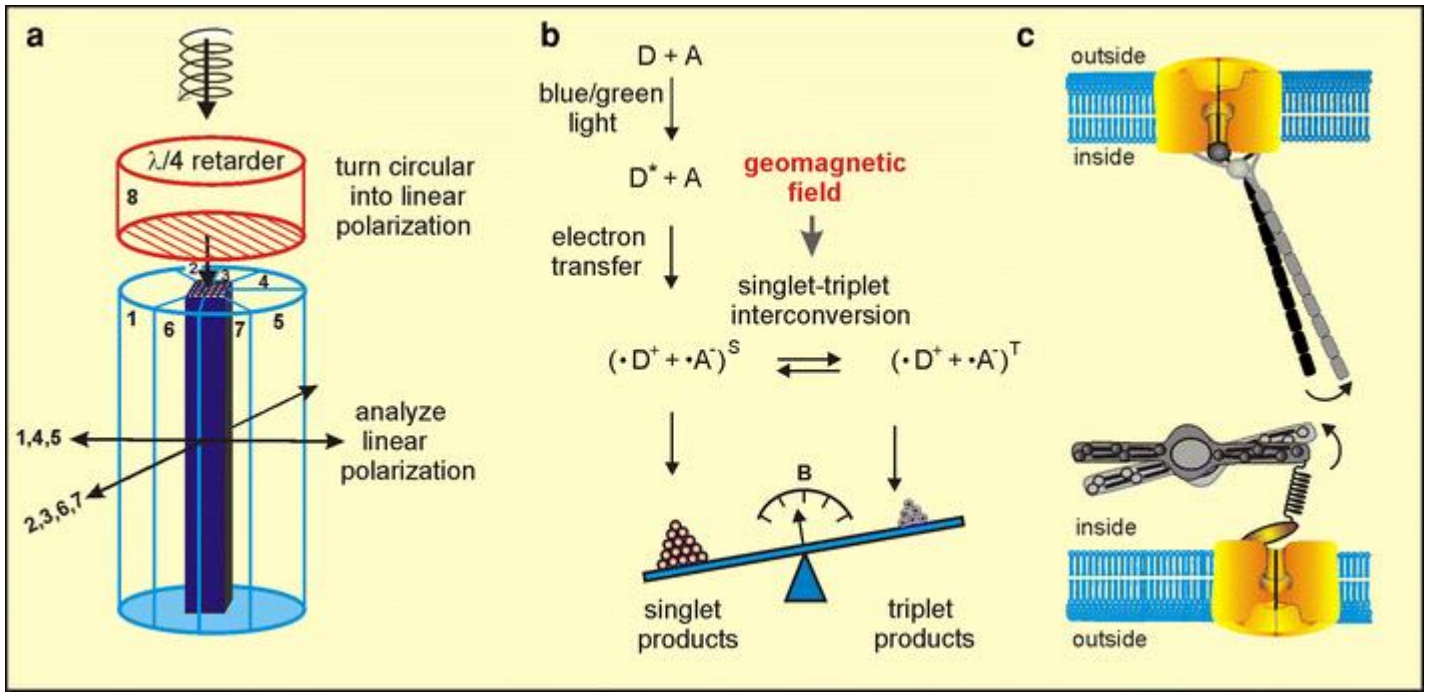






Primary processes in olfactory sensory cilia. Left: micrograph of an isolated olfactory receptor cell showing the chemosensory cilia at the ending of the neuron's dendrite (from: Kleene and Gesteland, 1981). Right current transduction model. AC adenylyl cyclase type III, ATP adenosine triphosphate, [Ca 2+] i intracellular calcium concentration, cAMP cyclic adenosine monophosphate, G olf olfactory GTP-binding protein, PDE phosphodiesterase. The two transduction channels, cAMP-gated cation channels and Ca2+-gated chloride channels, are indicated in the upper membrane. The ion transporters that extrude Ca2+ and accumulate Cl− are depicted at the bottom membrane of the cilium

Evaluating electromagnetic fields: more primary processes

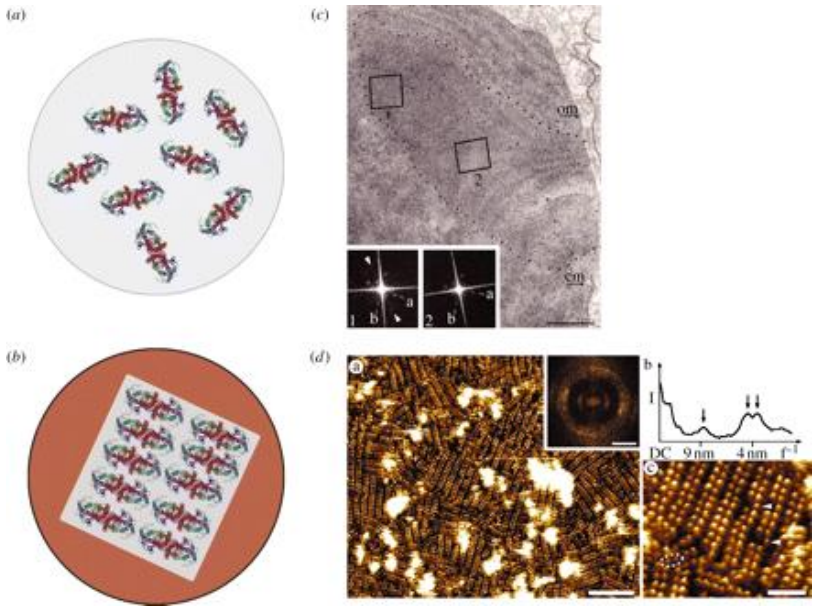


Primary processes in **polarization vision and magnetoreception** **a** Schematic representation of circular-polarization vision in the mantis shrimp. Photoreceptor 8 is positioned in the light path that enters an ommatidium. **The cell converts circularly polarized light into linearly polarized light**. The remaining seven photoreceptors analyze the polarization plane. (changed from Chiou et al. 2008). **b** The radical pair model of magnetoreception. Two domains of a cryptochrome molecule act as electron donor (D) and acceptor (**a**), respectively. Upon light absorption, the donor reaches the excited state D* and, subsequently, transfers an electron to the acceptor, **giving rise to a radical pair in a spin-correlated singlet state** $(\cdot D^+ + \cdot A^-)^S$. The yield of interconversions between the singlet and triplet states is affected by the geomagnetic field. The magnetosensory cell monitors the balance between singlet and triplet products as a measure of the magnetic field intensity B (changed from Ritz et al. 2000). **c** The magnetite hypothesis of magnetoreception. *Top* A chain **of single-domain magnetite particles is connected to the gating mechanism of an ion channel.** When the animal changes its position within the Earth's magnetic field, the chain is displaced and opens the channel. *Bottom* Small superparamagnetic magnetite particles are organized in plaques within the dendrite of a magnetosensitive neuron. These plaques consist of magnetite clusters (*spheres*) together with non-magnetic maghemite chains (*black lines*) around an iron-coated vesicle (*center*). The entire structure is thought to change its shape with its position in the geomagnetic field and to drive the gating mechanism of an ion channels through an elastic connection (changed from Solov'yov and Greiner 2007)

The atmosphere creates a pattern of celestial light that can be used for navigation

Moreover, reflective surfaces like water or glass, as well as scales, elythrae and other shiny animal surface structures, polarize light, an effect that can be used to search water, identify prey, and break other animals' camouflage (Kriska et al. 1998; Shashar et al. 2000). The primary transduction process of polarization vision is based on the photoreceptors with pronounced absorption anisotropy (dichroism). Such photoreceptors show a preferred response of their photosensitive organelles to polarized light with a certain electric vector (e-vector). The rhabdomeric photoreceptors of *insects and cephalopods harbor their rhodopsin in microvilli, membrane tubes of ~50 nm diameter. Apparently, the rotational freedom of rhodopsin is limited in the microvillar membrane, such that the orientation of the retinal molecules is mainly parallel to the long axis of the microvillus.*

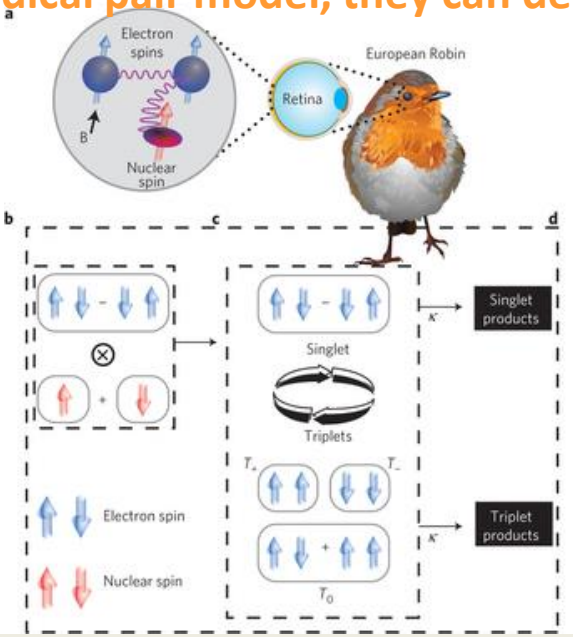
Polarized light is, therefore, best absorbed when its e-vector is aligned along the microvilli. Furthermore, all microvilli in a polarization-sensitive photoreceptor are aligned in parallel (Wehner and Bernard 1993; Meyer and Domanico 1999) so that the entire rhabdomer displays the same dichroism as each of its microvilli.

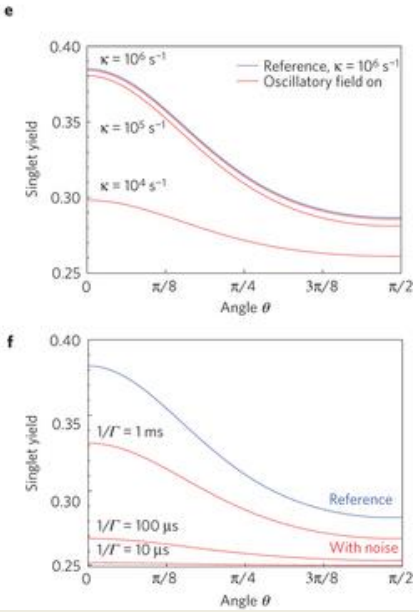


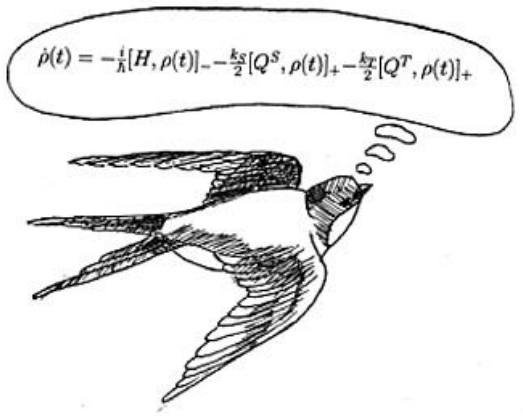
Potential lipid and protein interactions in ciliary photoreceptors. Schematics of (*a*) rod discs with opsin dimers still free to rotate versus (*b*) cone discs with phase separation into cholesterol-rich and more ordered (L_o, blue) and cholesterol-poor and more fluid (L_α, grey) domains, with dimers ordered into rows. Evidence for membrane phase separation from (*c*) cone transmission electron microscopy studies (adapted from [61]) and (*d*) rod AFM and *x*-ray diffraction studies (adapted from [49]).

The molecular basis of mechanisms underlying polarization vision
Nicholas W. Roberts, Megan L. Porter, Thomas W. Cronin
Published 31 January 2011.DOI: 10.1098/rstb.2010.0206

The radical pair model, they can determine spin interconversion caused by magnetic field.





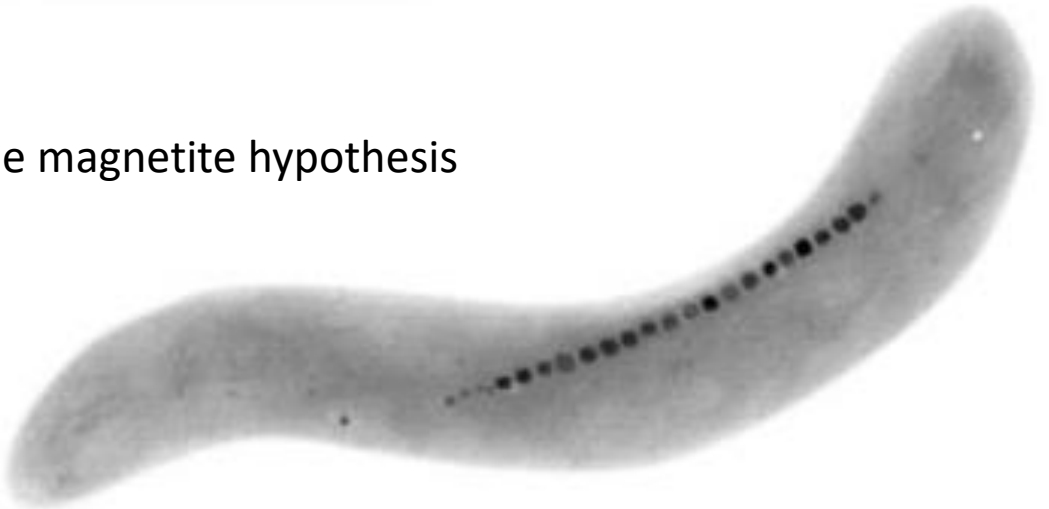


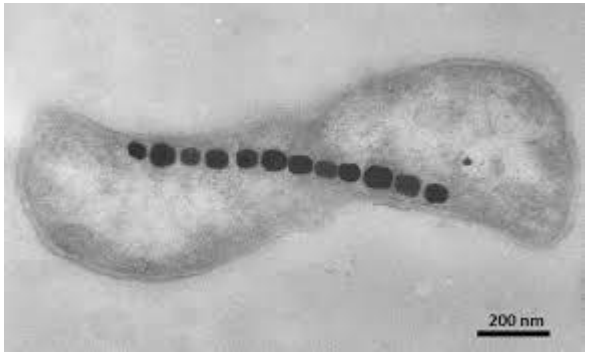
Animals can exploit at least three parameters of the magnetic field: the inclination of the magnetic field relative to the Earth's surface, and the direction to magnetic north, parameters that we obtain from an inclination compass and a declination compass, respectively. Moreover, animals perceive the local intensity of the geomagnetic field, a parameter that we determine using a magnetometer. In the search for the primary processes that transduce these parameters into neuronal signals, two models are currently favored, the ***radical pair model*** *and the magnetite hypothesis. The radical pair model is based on the observations that* ***certain modes of magnetoreception are light-dependent*** *(Ritz et al. 2002), and that* ***chemical free-radical reactions can be influenced by magnetic fields of ≤50 μT, the intensity of the geomagnetic field*** *(Maeda et al. 2008). The candidate biomolecule for such a light-induced, magneto-sensitive free-radical reaction is* ***cryptochrome****, a photopigment that is present in the* ***retina of migratory birds*** *(Möller et al. 2004) and was found to be necessary for* ***magnetoreception in Drosophila*** *(Gegear et al. 2008). Cryptochrome absorbs blue light and forms long-lived radical pairs (Liedvogel et al. 2007). The light-dependence of magnetoreception in birds has given rise to the notion that the impact of the magnetic field on cryptochrome photochemistry may represent a primary sensory process (Ritz et al. 2000, 2004; Beason 2005; Wiltschko and Wiltschko 2007).* ***The idea is that cryptochrome forms a singlet radical pair upon illumination, and that the kinetics of singlet/triplet interconversion is affected by the geomagnetic field (Fig. 8b).*** *The balance between singlet products and triplet products depends to some extent on the orientation of a cryptochrome-containing cell in the geomagnetic field. If a cryptochrome-containing cell is able to compare the amount of chemical products resulting from singlet pairs to that originating from triplet pairs, it can determine the yield of spin interconversion. Ritz et al. (2000) proposed that a visual representation of the magnetic field can result from* ***an ordered distribution of cryptochrome-containing cells in the retina.*** *While the radical pair model has not been established in all details, it represents a valuable hypothesis for directional magnetoreception in birds—it provides the molecular concept for a visual compass in the birds' eyes (Wiltschko and Wiltschko 2006).*

Quantum biology Neill Lambert, et al Nature Physics 9, 10–18 (2013) doi:10.1038/nphys2474

Positional information

Inclination of the magnetic field, the magnetite hypothesis (magnetotactic bacteria)





Animal physiologists have long speculated that magnetite particles may transduce geomagnetic signals in migratory animals (Kirschvink and Gould 1981; Kirschvink et al. 2001; Walker et al. 2002). Strings of permanently magnetic particles may be connected to the gating mechanism of an ion channel so that the magnetic field can trigger channel opening and generate a receptor potential (Fig. 8c). Indeed, single-domain magnetite particles were discovered in fish (Diebel et al. 2000), and indirect evidence points to a role of single-domain magnetite in magnetoreception by mole rats (Wegner et al. 2006) and bats (Holland et al. 2008). Curiously, the magnetite particles in various animals with robust magnetoreception are very small and are not aligned in orderly chains (e.g., homing pigeon; Fleissner et al. 2003). These particles have no stable magnetic moment, but they can assume a magnetic polarization in an applied field. An important recent finding is that such superparamagnetic material can, in principle, serve as a sensor in magnetosensory cells. Clusters of these particles change their shape when they are moved within a magnetic field (Fig. 8c). And the resulting forces are sufficient to gate ion channels (Fleissner et al. 2007; Hsu et al. 2007; Solov'yov and Greiner 2007). Thus, cryptochrome and magnetite may be the transducing molecules in directional and positional magnetoreception. This concept will be scrutinized and extended in the coming years with the still distant goal to understand magneto-electrical transduction in sensory neurons.

nature materials

Home | Current issue | Comment | Research | Archive ▾ | Authors & referees ▾ | About the journal ▾

home ▸ advance online publication ▸ full text

NATURE MATERIALS | ARTICLE

A magnetic protein biocompass

Siying Qin, Hang Yin, Celi Yang, Yunfeng Dou, Zhongmin Liu, Peng Zhang, He Yu, Yulong Huang, Jing Feng, Junfeng Hao, Jia Hao, Lizong Deng, Xiyun Yan, Xiaoli Dong, Zhongxian Zhao, Taijiao Jiang, Hong-Wei Wang, Shu-Jin Luo & Can Xie

Affiliations | Contributions | Corresponding author

Nature Materials (2015) | doi:10.1038/nmat4484

Received 04 August 2015 | Accepted 21 October 2015 | Published online 16 November 2015

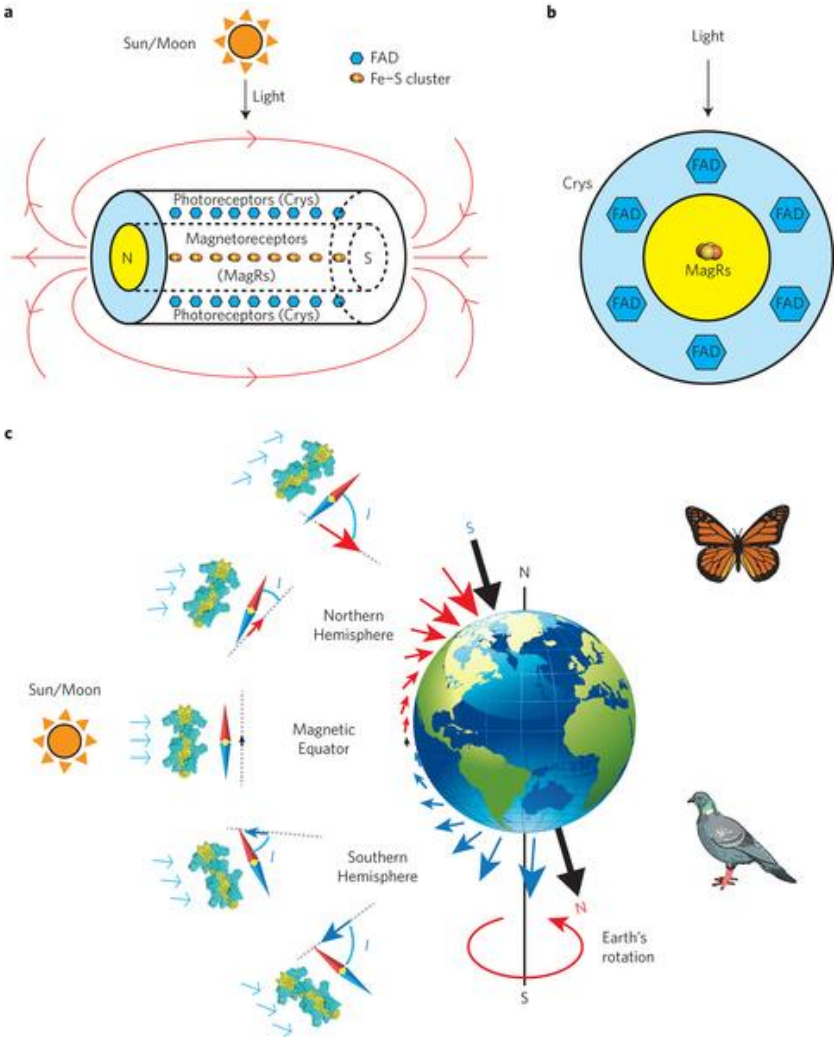
PDF | Citation | Reprints | Rights & permissions | Article metrics

Abstract

Abstract • Introduction • The biocompass model of magnetoreception • A genome-wide search for MagR • Experimental identification of MagR • Structural characterization of MagR and Cry/MagR • Molecular modelling of Cry/MagR complex structure • Expression of MagR and Cry co-localized in the retina • Intrinsic magnetic moment of MagR and Cry/MagR • Outlook • Methods • References • Acknowledgements • Author information • Supplementary information

The notion that animals can detect the Earth's magnetic field was once ridiculed, but is now well established. Yet the biological nature of such magnetosensing phenomenon remains unknown. Here, we report a putative magnetic receptor (*Drosophila* CG8198, here named MagR) and a multimeric magnetosensing rod-like protein complex, identified by theoretical postulation and genome-wide screening, and validated with cellular, biochemical, structural and biophysical methods. The magnetosensing complex consists of the identified putative magnetoreceptor and known magnetoreception-related photoreceptor cryptochromes (Cry), has the attributes of both Cry- and iron-based systems, and exhibits spontaneous alignment in magnetic fields, including that of the Earth. Such a protein complex may form the basis of magnetoreception in animals, and may lead to applications across multiple fields.

Subject terms: Biological physics • Biomaterials • Biophysics • Physiology • Structural biology

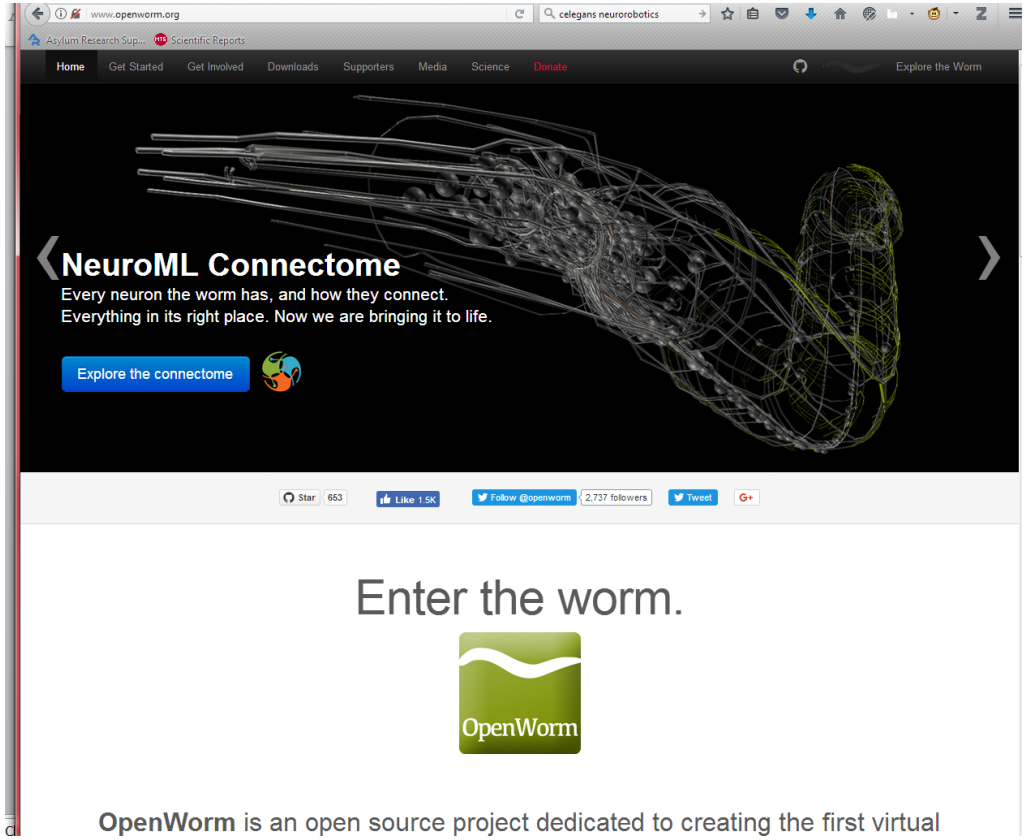


, A nanoscale Cry/MagR magnetosensor complex with intrinsic magnetic polarity acts as a light-dependent biocompass. Linear polymerization of Fe–S cluster-containing magnetoreceptors (MagR) leads to the formation of a rod-like biocompass at the centre (core, yellow), surrounded by photoreceptive cryptochromes (Cry; outer layer, cyan). b, Cross-section of a, indicating that electron transportation from the FAD group in Cry to the Fe–S cluster in MagR upon light stimulation may be possible. c, The biocompass model of magnetoreception. In animal navigation systems, the Cry/MagR magnetosensor complex may act as a biological compass that perceives information from the Earth's geomagnetic field, such as polarity (as with a conventional compass), intensity and inclination. The surface representation of the Cry/MagR structure (cyan and yellow) has been validated by EM in this study (Figs 2 and 3). The intrinsic magnetic moment of the magnetosensor may form a polarity compass for the sensing of directional information from the Earth's geomagnetic field. The capability to detect the intensity and the spontaneous alignment of the magnetosensor in magnetic fields (as shown on the left-hand side, and further elucidated in Fig. 5a, b), may form the basis of an intensity sensor and inclination compass. Earth's magnetic poles (black arrows) are offset from the axis of rotation (black line). The inclination angle (labelled as 'I') and intensity of the field are indicated by the direction and length of the arrows (red in the Northern Hemisphere and blue in the Southern Hemisphere). MagR and Cry/MagR magnetosensors from two species, monarch butterfly (Danaus plexippus, upper right) and pigeon (Columba livia, lower right), were tested in this study, highlighting the evolutionarily conserved biocompass model

Deep learning artificial intelligence, hierarchical arrangements of neurons and sensors

Why does deep and cheap learning work so well?

Henry W. Lin (Harvard), Max Tegmark (MIT)
(Submitted on 29 Aug 2016 (v1), last revised 28 Sep 2016 (this version, v2))
We show how the success of deep learning depends not only on mathematics but also on physics: although well-known mathematical theorems guarantee that neural networks can approximate arbitrary functions well, the class of functions of practical interest can be approximated through "cheap learning" with exponentially fewer parameters than generic ones, because they have simplifying properties tracing back to the laws of physics. The exceptional simplicity of physics-based functions hinges on properties such as symmetry, locality, compositionality and polynomial log-probability, and we explore how these properties translate into exceptionally simple neural networks approximating both natural phenomena such as images and abstract representations thereof such as drawings. We further argue that when the statistical process generating the data is of a certain hierarchical form prevalent in physics and machine-learning, a deep neural network can be more efficient than a shallow one. We formalize these claims using information theory and discuss the relation to renormalization group procedures. We prove various "no-flattening theorems" showing when such efficient deep networks cannot be accurately approximated by shallow ones without efficiency loss: flattening even linear functions can be costly, and flattening polynomials is exponentially expensive; we use group theoretic techniques to show that n variables cannot be multiplied using fewer than 2^n neurons in a single hidden layer.


www.openworm.org
celegans neurorobotics
Asylum Research Sup...
Scientific Reports
Home
Get Started
Get Involved
Downloads
Supporters
Media
Science
Donate
Explore the Worm
NeuroML Connectome
Every neuron the worm has, and how they connect.
Everything in its right place. Now we are bringing it to life.
Explore the connectome
Star 653
Like 1.5K
Follow @openworm 2,737 followers
Tweet
G+
Enter the worm.
OpenWorm
OpenWorm is an open source project dedicated to creating the first virtual

